

Nonadiabatic tunneling in circularly polarized laser fields: Derivation of formulas

Ingo Barth¹ and Olga Smirnova¹

¹*Max Born Institute, Max-Born-Str. 2A, 12489, Berlin, Germany*

(Dated: January 22, 2018)

Abstract

We provide detailed analysis of strong field ionization of degenerate valence p orbitals by circularly polarized fields. Our analytical approach is conceptually equivalent to the Perelomov, Popov, and Terent'ev (PPT) theory and is virtually exact for short range potentials. After benchmarking our results against the PPT theory for s orbitals, we obtain the results for p orbitals. We also show that, as long as the dipole approximation is valid, both the PPT method and our results are gauge invariant, in contrast with widely used strong field approximation (SFA). Our main result, which has already been briefly outlined in [I. Barth and O. Smirnova, Phys. Rev. A **84**, 063415 (2011)], is that strong field ionization preferentially removes electrons counter-rotating to the circularly polarized laser field. The result is illustrated using the example of Kr atom. Strong, up to one order of magnitude, sensitivity of strong field ionization to the sense of electron rotation in the initial state is one of the key signatures of non-adiabatic regime of strong field ionization.

PACS numbers: 42.50.Hz, 32.80.Rm, 33.80.Wz

I. INTRODUCTION

The analysis of ionization in strong low-frequency laser fields is often based on adiabatic approximation. In this approximation, ionization is treated as tunneling through a static (or quasi-static) barrier created by the binding potential and the voltage drop due to the electric field of the laser pulse. This picture implies that the electron does not see the oscillations of the low-frequency laser field during ionization, i.e. tunneling happens “faster” than the oscillation of linear or the rotation of circular field. Formally, this picture corresponds to the limit $\gamma \ll 1$, where $\gamma = \sqrt{2I_p}\omega/\mathcal{E}$ is the Keldysh parameter [1], I_p is the ionization potential, ω is the laser frequency, and \mathcal{E} is the strength of the laser field.

However, for typical experimental conditions, both for linear and for circularly polarized fields [2–7], the Keldysh parameter is often in the non-adiabatic tunneling regime [8, 9], i.e. $\gamma \sim 1$. Therefore, the adiabatic-based interpretation of these experiments is questionable. In particular, we have shown in Ref. [10] that for strong field ionization in circularly polarized laser fields, the sense of electron rotation becomes significant already for $\gamma < 1$, i.e. even when using longer-wavelength laser radiation than the standard 800 nm, e.g. 1300 nm as in Ref. [5]. As a consequence of non-adiabatic effects, the counter-rotating electron can have up to one order of magnitude larger ionization rate than co-rotating, depending on the laser field parameters. Our theoretical prediction has now been confirmed by the experiment [11].

The goal of this paper is to expose our calculations and discuss the approximations we have used in deriving simple formulas for ionization rates presented in Ref. [10]. We follow the theory developed by Perelomov, Popov, and Terent’ev (PPT) [12, 13] for short range potentials and apply it to p orbitals. Including effects of the long-range Coulomb potential in a standard way [14, 15] and including non-adiabatic Coulomb effects [16, 17] do not change our conclusions. The Stark shift of the initial state is not included in our analysis, but it can be calculated separately [7, 18] and used to correct the field-free ionization potential used in the present calculation.

The key advantage of the PPT approach is its gauge invariance, which is discussed below in the paper. The violation [19–21] of gauge invariance in strong field approximation (SFA) leads to both technical and conceptual problems [22]. In particular, for the ionization of p orbitals by strong circularly polarized fields, the SFA yields inconsistent results in both gauges [23, 24], which contradict experimental measurements of either ionization yields [11]

or electron spectra (see e.g. Refs. [2–4, 6, 7]). Note that in linearly polarized fields the length gauge SFA and the PPT theory yield equivalent results for short range potentials [25]. The results of length gauge SFA and the PPT are different if long range effects are taken into account, with length gauge SFA leading to incorrect prefactor of ionization rate [1]. The deficiencies of velocity gauge SFA are well documented [19–21] and are significant even for short range potentials, e.g. velocity gauge SFA predicts identical total ionization rates from p_+ and p_- orbitals [23].

Our analysis reveals that optimal quantum trajectory, which minimizes electron action under the barrier, corresponds to initial non-zero lateral velocity in direction opposite to the rotation of the laser field. The weight of this trajectory is determined by the direction of electron current in the initial orbital and is higher for p_- orbitals in case of right circular polarization of the laser field.

Finally, we show that non-adiabatic dynamics of strong field ionization leads to non-trivial rotational dynamics of the hole left in the ion. This dynamics leads to the generation of electronic ring currents in ions [26, 27], and the coherence of this dynamics can be probed with attosecond time-resolution using attosecond transient absorption technique demonstrated recently in Ref. [28].

This paper is organized as follows: In Section II, we derive analytical formulas for the ionization rates based on the PPT theory. We first benchmark our results for s orbitals against the PPT results [12]. We then derive the results for p_0 and p_{\pm} orbitals. In Section III, we apply these formulas to the strong field ionization of the Kr atom. Section IV concludes this work.

II. THEORY

A. Ionization model in circularly polarized laser fields

The PPT formulas for the atomic ionization rates were derived for the strong field ionization in linearly, circularly, and elliptically polarized laser fields [12, 13]. However, for circular and elliptical polarizations, there are formulas only for s orbitals. In this section, we derive the analytical formula for the ionization rates in circularly polarized laser fields also for p_m orbitals with azimuthal quantum numbers $m = 0, \pm 1$. The right (+) or left (−) circularly

polarized laser field is defined as

$$\mathbf{E}_\pm(t) = \mathcal{E} (\cos(\omega t) \mathbf{e}_x \pm \sin(\omega t) \mathbf{e}_y), \quad (1)$$

which is connected with the vector potential

$$\mathbf{A}_\pm(t) = -A_0 (\sin(\omega t) \mathbf{e}_x \mp \cos(\omega t) \mathbf{e}_y) \quad (2)$$

by the relation $\mathbf{E}_\pm(t) = -d\mathbf{A}_\pm(t)/dt$, where \mathcal{E} is the electric field amplitude, $A_0 = \mathcal{E}/\omega$ is the velocity amplitude of the electron oscillations in the laser field, and ω is the laser frequency.

We assume that the electron ionization from the valence p shell is described by the time-dependent Schrödinger equation (TDSE) in single active electron model within dipole approximation

$$i \frac{\partial}{\partial t} \psi_\pm(\mathbf{r}, t) = \left[-\frac{\nabla_{\mathbf{r}}^2}{2} + V(\mathbf{r}) + \mathbf{r} \cdot \mathbf{E}_\pm(t) \right] \psi_\pm(\mathbf{r}, t), \quad (3)$$

where $V(\mathbf{r})$ is the effective potential and the atomic units are used throughout in this work. The exact solution of this TDSE is the integral equation for the time-dependent wavefunction $\psi_\pm(\mathbf{r}, t)$ starting at time t_0 [12]

$$\psi_\pm(\mathbf{r}, t) = \int d\mathbf{r}' G_\pm(\mathbf{r}, t, \mathbf{r}', t_0) \psi_\pm(\mathbf{r}', t_0) - i \int_{t_0}^t dt_i \int d\mathbf{r}' G_\pm(\mathbf{r}, t, \mathbf{r}', t_i) V(\mathbf{r}') \psi_\pm(\mathbf{r}', t_i), \quad (4)$$

where

$$G_\pm(\mathbf{r}, t, \mathbf{r}', t_i) = \frac{\theta(t - t_i)}{(2\pi)^3} \int d\mathbf{k} e^{i\mathbf{v}_\pm(t)\mathbf{r} - i\mathbf{v}_\pm(t_i)\mathbf{r}'} e^{-\frac{i}{2} \int_{t_i}^t \mathbf{v}_\pm(\tau)^2 d\tau} \quad (5)$$

is the Green's function of the electron for motion in a circularly polarized field,

$$\mathbf{v}_\pm(t) = \mathbf{k} + \mathbf{A}_\pm(t) \quad (6)$$

is the instantaneous electron velocity, and \mathbf{k} is the final momentum observed at the detector. Moreover, we divide $\mathbf{k} = \mathbf{k}_\parallel + \mathbf{k}_\perp$ into two components $\mathbf{k}_\parallel = k_x \mathbf{e}_x + k_y \mathbf{e}_y$ and $\mathbf{k}_\perp = k_z \mathbf{e}_z$, which are parallel ($\mathbf{k}_\parallel \parallel \mathbf{A}_\pm(t)$) and perpendicular ($\mathbf{k}_\perp \perp \mathbf{A}_\pm(t)$) to the laser field, respectively.

The first term of Eq. (4) does not contribute to the ionization rate, because it describes

the smearing out of the initial state [12]. As in PPT theory, the main approximation of this theory is the neglect of the distortion of the initial wavefunction $\psi_{\pm}(\mathbf{r}', t_i)$ by Stark effect prior to ionization at time t_i , i.e. we replace the exact wavefunction $\psi_{\pm}(\mathbf{r}', t_i)$ on the right side of Eq. (4) by the wavefunction of the bound orbital for the free atom $\varphi_{lm}(\mathbf{r}')e^{iI_p t_i}$ with quantum numbers l , m and ionization potential I_p . Using the field-free TDSE, the term $V(\mathbf{r}')\psi_{\pm}(\mathbf{r}', t_i)$ is replaced by

$$V(\mathbf{r}')\varphi_{lm}(\mathbf{r}')e^{iI_p t_i} = \frac{1}{2}(\nabla_{\mathbf{r}'}^2 - 2I_p)\varphi_{lm}(\mathbf{r}')e^{iI_p t_i}. \quad (7)$$

As already described in Ref. [12] in detail, the difference between two wavefunctions $\psi_{\pm}(\mathbf{r}', t_i)$ and $\varphi_{lm}(\mathbf{r}')e^{iI_p t_i}$ is small for short-range potentials, i.e. the potential $V(\mathbf{r})$ falls more rapidly than the effective Coulomb potential $\sim 1/r$. However, the Coulomb corrections can be introduced using standard recipes [14, 15] involving the time-integration of the Coulomb potential along the optimal trajectory. In this work, we use the short-range potential and will include Coulomb corrections in our future work.

Furthermore, we assume that the laser field is turned on at $t_0 \rightarrow -\infty$ adiabatically. Then, using the momentum representation of the wavefunction

$$\tilde{\varphi}_{lm}(\mathbf{k}) = \frac{1}{(2\pi)^{3/2}} \int d\mathbf{r} e^{-i\mathbf{k}\mathbf{r}} \varphi_{lm}(\mathbf{r}) \quad (8)$$

and the abbreviation

$$\phi_{lm}(\mathbf{v}_{\pm}(t)) = \frac{1}{2}(\mathbf{v}_{\pm}(t)^2 + 2I_p)\tilde{\varphi}_{lm}(\mathbf{v}_{\pm}(t)), \quad (9)$$

we get the approximative electron wavefunction from Eq. (4)

$$\psi_{\pm}(\mathbf{r}, t) = \frac{i}{(2\pi)^{3/2}} \int_{-\infty}^t dt_i e^{iI_p t_i} \int d\mathbf{k} e^{i\mathbf{v}_{\pm}(t)\mathbf{r}} e^{-\frac{i}{2} \int_{t_i}^t \mathbf{v}_{\pm}(\tau)^2 d\tau} \phi_{lm}(\mathbf{v}_{\pm}(t_i)). \quad (10)$$

For circularly polarized fields, it is advantageous to use cylindrical coordinates (ρ, ϕ, z) instead of Cartesian ones (x, y, z) in coordinate space related by $x = \rho \cos \phi$ and $y = \rho \sin \phi$. Similarly, we introduce cylindrical coordinates (k_{ρ}, θ, k_z) in momentum space with relations $k_x = k_{\rho} \cos \theta$ and $k_y = k_{\rho} \sin \theta$, thus $k_{\rho}^2 = k_x^2 + k_y^2 = k_{\parallel}^2$ and $k^2 = k_{\rho}^2 + k_z^2 = k_{\parallel}^2 + k_{\perp}^2$. With

Eqs. (2) and (6), two exponents in Eq. (10) are expressed as

$$i\mathbf{v}_{\pm}(t)\mathbf{r} = if_{\pm}(k_{\rho}, \theta, \phi, t)\rho + ik_z z \quad (11)$$

and

$$-\frac{i}{2} \int_{t_i}^t \mathbf{v}_{\pm}(\tau)^2 d\tau = -\frac{i}{2} (k^2 + A_0^2) (t - t_i) - i\mathbf{k}(\boldsymbol{\xi}_{\pm}(t) - \boldsymbol{\xi}_{\pm}(t_i)), \quad (12)$$

where

$$f_{\pm}(k_{\rho}, \theta, \phi, t) = k_{\rho} \cos(\theta - \phi) - A_0 \sin(\omega t \mp \phi) \quad (13)$$

and

$$\boldsymbol{\xi}_{\pm}(t) = \mathbf{E}_{\pm}(t)/\omega^2. \quad (14)$$

B. Derivation of the formula for the time-averaged ionization rate

We follow the derivation of the formula for the ionization rate in Refs. [12, 13] based on the PPT approach and repeat it here for clarification and only for the case of circular polarization ($\varepsilon = 1$). The time-averaged ionization rate $w_{\pm}(\mathcal{E}, \omega)$ is equal to the time-averaged radial flux at the infinity $\rho \rightarrow \infty$, i.e.

$$w_{\pm}(\mathcal{E}, \omega) = \lim_{\rho \rightarrow \infty} \overline{J_{\pm}(\rho, t)}. \quad (15)$$

The radial flux $J_{\pm}(\rho, t)$ is evaluated as the integral of the radial component of the flux density $j_{\rho\pm}(\mathbf{r}, t)$ over a cylinder of radius ρ with its axis along the propagation z -axis of the circularly polarized laser field, i.e.

$$J_{\pm}(\rho, t) = \rho \int_{-\infty}^{\infty} dz \int_0^{2\pi} d\phi j_{\rho\pm}(\rho, \phi, z, t), \quad (16)$$

where $j_{\rho\pm}(\mathbf{r}, t)$ is defined as

$$j_{\rho\pm}(\mathbf{r}, t) = \frac{i}{2} \left(\psi_{\pm}(\mathbf{r}, t) \frac{\partial}{\partial \rho} \psi_{\pm}^*(\mathbf{r}, t) - \psi_{\pm}^*(\mathbf{r}, t) \frac{\partial}{\partial \rho} \psi_{\pm}(\mathbf{r}, t) \right). \quad (17)$$

Inserting Eqs. (10)–(12) into Eq. (17), we get

$$j_{\rho\pm}(\mathbf{r}, t) = \frac{1}{2(2\pi)^3} \int d\mathbf{k}_1 \int d\mathbf{k}_2 e^{i(\mathbf{k}_2 - \mathbf{k}_1)(\mathbf{r} - \boldsymbol{\xi}_{\pm}(t))} (f_{\pm}(k_{1\rho}, \theta_1, \phi, t) + f_{\pm}(k_{2\rho}, \theta_2, \phi, t)) \quad (18)$$

$$\int_{-\infty}^t dt_{1i} e^{\frac{i}{2}(k_1^2 + A_0^2 + 2I_p)(t - t_{1i})} F_{\pm}^*(\mathbf{k}_1, t_{1i}) \int_{-\infty}^t dt_{2i} e^{-\frac{i}{2}(k_2^2 + A_0^2 + 2I_p)(t - t_{2i})} F_{\pm}(\mathbf{k}_2, t_{2i}),$$

where the function

$$F_{\pm}(\mathbf{k}, t) = \phi_{lm}(\mathbf{v}_{\pm}(t)) e^{i\mathbf{k}\boldsymbol{\xi}_{\pm}(t)} \quad (19)$$

contains terms with complicated, but periodic time-dependence. Expanding $F_{\pm}(\mathbf{k}, t)$ into the Fourier series

$$F_{\pm}(\mathbf{k}, t) = \sum_{n=-\infty}^{\infty} F_{n\pm}(\mathbf{k}, \omega) e^{-in\omega t} \quad (20)$$

with the Fourier coefficients

$$F_{n\pm}(\mathbf{k}, \omega) = \frac{1}{2\pi} \int_{-\pi}^{\pi} d(\omega t) F_{\pm}(\mathbf{k}, t) e^{in\omega t} \quad (21)$$

and carrying out time-integrations in Eq. (18), according to ($a \in \mathbb{R}, \delta > 0$)

$$\int_{-\infty}^t dt' e^{\pm ia(t-t')} = \lim_{\delta \rightarrow 0} \frac{\pm i}{a \pm i\delta}, \quad (22)$$

yields the final formula for the radial component of the flux density ($\delta > 0$)

$$j_{\rho\pm}(\mathbf{r}, t) = \lim_{\delta \rightarrow 0} \frac{1}{2(2\pi)^3} \int d\mathbf{k}_1 \int d\mathbf{k}_2 e^{i(\mathbf{k}_2 - \mathbf{k}_1)(\mathbf{r} - \boldsymbol{\xi}_{\pm}(t))} (f_{\pm}(k_{1\rho}, \theta_1, \phi, t) + f_{\pm}(k_{2\rho}, \theta_2, \phi, t)) \quad (23)$$

$$\sum_{n_1=-\infty}^{\infty} F_{n_1\pm}^*(\mathbf{k}_1, \omega) \left[\frac{k_1^2}{2} + \frac{A_0^2}{2} + I_p - n_1\omega + i\delta \right]^{-1}$$

$$\sum_{n_2=-\infty}^{\infty} F_{n_2\pm}(\mathbf{k}_2, \omega) \left[\frac{k_2^2}{2} + \frac{A_0^2}{2} + I_p - n_2\omega - i\delta \right]^{-1} e^{-i(n_2 - n_1)\omega t}.$$

This expression is then inserted into the formula for the the radial flux $J_{\pm}(\rho, t)$, Eq. (16).

With

$$i(\mathbf{k}_2 - \mathbf{k}_1)\mathbf{r} = i\rho((k_{2x} - k_{1x}) \cos \phi + (k_{2y} - k_{1y}) \sin \phi) + i(k_{2z} - k_{1z})z, \quad (24)$$

the z -integration is easily carried out, i.e.

$$\int_{-\infty}^{\infty} dz e^{i(\mathbf{k}_2 - \mathbf{k}_1)\mathbf{r}} = 2\pi\delta(k_{2z} - k_{1z})e^{i\rho((k_{2x} - k_{1x})\cos\phi + (k_{2y} - k_{1y})\sin\phi)}. \quad (25)$$

But the evaluation of the ϕ -integration is challenging. Using Eq. (13), the Euler's formula, and the substitution $|\mathbf{k}_{2\parallel} - \mathbf{k}_{1\parallel}| \sin\phi' = (k_{2x} - k_{1x})\cos\phi + (k_{2y} - k_{1y})\sin\phi$, the ϕ -integral is evaluated as (see Appendix 1)

$$\begin{aligned} & \int_0^{2\pi} d\phi e^{i\rho((k_{2x} - k_{1x})\cos\phi + (k_{2y} - k_{1y})\sin\phi)} (f_{\pm}(k_{1\rho}, \theta_1, \phi, t) + f_{\pm}(k_{2\rho}, \theta_2, \phi, t)) \\ &= 2\pi i (k_{2\rho}^2 - k_{1\rho}^2 - 2k_{2\rho}A_0 \sin(\omega t \mp \theta_2) + 2k_{1\rho}A_0 \sin(\omega t \mp \theta_1)) \frac{J_1(\rho|\mathbf{k}_{2\parallel} - \mathbf{k}_{1\parallel}|)}{|\mathbf{k}_{2\parallel} - \mathbf{k}_{1\parallel}|}, \end{aligned} \quad (26)$$

where $J_n(x)$ is the Bessel function of the first kind, cf. Ref. [13]. Then, we carry out the simple integration over k_{1z} and get the result for the radial flux

$$\begin{aligned} J_{\pm}(\rho, t) &= \lim_{\delta \rightarrow 0} \frac{i}{\pi} \int d\mathbf{k}_{1\parallel} \int d\mathbf{k}_{2\parallel} e^{-i(\mathbf{k}_{2\parallel} - \mathbf{k}_{1\parallel})\xi_{\pm}(t)} \\ & (k_{2\rho}^2 - k_{1\rho}^2 - 2k_{2\rho}A_0 \sin(\omega t \mp \theta_2) + 2k_{1\rho}A_0 \sin(\omega t \mp \theta_1)) \frac{\rho J_1(\rho|\mathbf{k}_{2\parallel} - \mathbf{k}_{1\parallel}|)}{|\mathbf{k}_{2\parallel} - \mathbf{k}_{1\parallel}|} \\ & \int_{-\infty}^{\infty} dk_z \sum_{n_1=-\infty}^{\infty} F_{n_1\pm}^*((\mathbf{k}_{1\parallel}, k_z), \omega) [k_{1\rho}^2 + k_z^2 + A_0^2 + 2I_p - 2n_1\omega + i\delta]^{-1} \\ & \sum_{n_2=-\infty}^{\infty} F_{n_2\pm}((\mathbf{k}_{2\parallel}, k_z), \omega) [k_{2\parallel}^2 + k_z^2 + A_0^2 + 2I_p - 2n_2\omega - i\delta]^{-1} e^{-i(n_2 - n_1)\omega t}. \end{aligned} \quad (27)$$

To obtain the limit of the radial flux at the infinity $\rho \rightarrow \infty$, we apply the relation for the arbitrary function $g(\mathbf{k}_{\parallel})$ (see Appendix 2)

$$\lim_{\rho \rightarrow \infty} \int d\mathbf{k}_{\parallel} g(\mathbf{k}_{\parallel}) \frac{\rho J_1(\rho k_{\parallel})}{k_{\parallel}} = 2\pi \int d\mathbf{k}_{\parallel} g(\mathbf{k}_{\parallel}) \delta(\mathbf{k}_{\parallel}), \quad (28)$$

cf. Ref. [13], carry out the integration of the radial flux over k_{1y} , and use Eqs. (1), (14), and the substitutions $k_{\pm} = k_{2x} \pm k_{1x}$. Then, the intermediate result is

$$\begin{aligned} \lim_{\rho \rightarrow \infty} J_{\pm}(\rho, t) &= \lim_{\delta \rightarrow 0} i \int_{-\infty}^{\infty} dk_- \delta(k_-) k_- e^{-\frac{iA_0 k_-}{\omega} \cos(\omega t)} \\ & \int_{-\infty}^{\infty} dk_y \int_{-\infty}^{\infty} dk_z \sum_{n_1=-\infty}^{\infty} \sum_{n_2=-\infty}^{\infty} e^{-i(n_2 - n_1)\omega t} \int_{-\infty}^{\infty} dk_+ h_{\pm}(k_+) \end{aligned} \quad (29)$$

$$\left[\frac{1}{4}(k_+ - k_-)^2 + k_y^2 + k_z^2 + A_0^2 + 2I_p - 2n_1\omega + i\delta \right]^{-1} \\ \left[\frac{1}{4}(k_+ + k_-)^2 + k_y^2 + k_z^2 + A_0^2 + 2I_p - 2n_2\omega - i\delta \right]^{-1},$$

where the analytical function $h(k_+)$ is defined as

$$h_{\pm}(k_+) = (k_+ - 2A_0 \sin(\omega t)) F_{n_1 \pm}^* \left(\left(\frac{k_+ - k_-}{2}, k_y, k_z \right), \omega \right) F_{n_2 \pm} \left(\left(\frac{k_+ + k_-}{2}, k_y, k_z \right), \omega \right). \quad (30)$$

It is now shown in Eqs. (29) and (30), that the ionization rate depends on the sense (\pm) of circular polarization only in the function $F_{\pm}(\mathbf{k}, t)$, Eq. (19). By further deep analysis, the k_+ -integrand in Eq. (29) has four poles whose locations on the complex plane and corresponding residues depend particularly on n_1 and n_2 . For $k_- = 0$ and $0 \neq n_1 \neq n_2 \neq 0$, all four residues are finite, thus the k_- -integral in Eq. (29) would be zero due to the appearance of the factor k_- in the integrand. Therefore, the condition for the number of photons $n = n_1 = n_2$ must be satisfied. Furthermore, for $2n\omega < k_y^2 + k_z^2 + A_0^2 + 2I_p$, there are only two residues that could contribute to the ionization rate, but in the limit $k_- = 0$ these residues are opposite. Therefore, we consider only the case $2n\omega \geq k_y^2 + k_z^2 + A_0^2 + 2I_p$, where only two residues contribute to the ionization rate. By the way, we denote the quantity n_0 as the minimal number of photons required for ionization in circularly polarized laser fields, i.e.

$$n_0 = \frac{A_0^2}{2\omega} + \frac{I_p}{\omega} = \frac{2U_p + I_p}{\omega}, \quad (31)$$

where $U_p = A_0^2/4$ is the pondermotive potential. Comparing to the case for linearly polarized laser fields, the mean kinetic energy of the electron in a circularly polarized laser field $A_0^2/2 = 2U_p$ is twice as much. Applying the residue method for the k_+ -integral and evaluating the k_- -integral, we get the expression for the radial flux at the infinity (see Appendix 3)

$$\lim_{\rho \rightarrow \infty} J_{\pm}(\rho, t) = \pi \sum_{n \geq n_0}^{\infty} \int_{-\infty}^{\infty} dk_y \int_{-\infty}^{\infty} dk_z \frac{h_{\pm}(2\sqrt{k_n^2 - k_y^2 - k_z^2}) - h_{\pm}(-2\sqrt{k_n^2 - k_y^2 - k_z^2})}{k_n^2 - k_y^2 - k_z^2}, \quad (32)$$

where

$$\frac{k_n^2}{2} = (n - n_0)\omega. \quad (33)$$

Using Eq. (30) for $k_- = 0$ and $n = n_1 = n_2$, i.e.

$$h_{\pm}(k_+) = (k_+ - 2A_0 \sin(\omega t)) \left| F_{n_{\pm}} \left(\left(\frac{k_+}{2}, k_y, k_z \right), \omega \right) \right|^2, \quad (34)$$

time-averaging over a laser cycle, and using the relations for the δ function $\delta(\alpha^2 - x^2) = [\delta(\alpha - x) + \delta(\alpha + x)]/(2|\alpha|)$ and $\delta(\alpha x) = \delta(x)/|\alpha|$, we obtain the final formula for the ionization rate from Eq. (15) as a sum over multiphoton channels

$$w_{\pm}(\mathcal{E}, \omega) = \sum_{n \geq n_0}^{\infty} w_{n_{\pm}}(\mathcal{E}, \omega), \quad (35)$$

and

$$w_{n_{\pm}}(\mathcal{E}, \omega) = 2\pi \int d\mathbf{k} \delta \left(\frac{k^2}{2} - \frac{k_n^2}{2} \right) |F_{n_{\pm}}(\mathbf{k}, \omega)|^2, \quad (36)$$

which coincide exactly with Eqs. (13) and (14) of Ref. [13] for circular polarization, respectively. In Eq. (36), we recognize that there is the conservation law, namely $k = k_n$, that means that the electron kinetic energy is equal the photon energy minus the mean electron energy in a circularly polarized laser field and the ionization energy, cf. Eqs. (31) and (33), i.e.

$$\frac{k^2}{2} = \frac{k_n^2}{2} = n\omega - 2U_p - I_p. \quad (37)$$

C. Gauge invariance

The length gauge was used in the derivation as in the original PPT approach. However, we note that the result for ionization rate is independent of the gauge. Rewriting Eqs. (3)–(5) using the velocity gauge yields substitution of the original wavefunction $\psi_{\pm}(\mathbf{r}, t)$ in the length gauge by $\psi_{\pm}(\mathbf{r}, t)e^{-i\mathbf{A}_{\pm}(t)\mathbf{r}}$ in Eq. (10). Thus, in right hand side of Eq. (10) the term $e^{i\mathbf{v}_{\pm}(t)\mathbf{r}}$ is then replaced by $e^{i\mathbf{v}_{\pm}(t)\mathbf{r}}e^{-i\mathbf{A}_{\pm}(t)\mathbf{r}} = e^{i\mathbf{k}\mathbf{r}}$ and the function in Eq. (13) is therefore time-independent, i.e. $f_{\pm}(k_{\rho}, \theta, \phi) = k_{\rho} \cos(\theta - \phi)$. Following the derivation in the previous section, Eqs. (26) and (30) do not have any time-dependent terms anymore, yielding the time-independent radial flux in Eq. (32). Therefore, time-averaging over a laser cycle is unnecessary in the velocity gauge, yielding the same result for the ionization rate as in

Eqs. (35) and (36).

D. Derivation of the formula for the probability of the n -photon process

The function $|F_{n\pm}(\mathbf{k}, \omega)|^2$ in Eq. (36) describes the probability of the n -photon process in circularly polarized fields, which is derived in this work not only for s - but also for all atomic orbitals, thus beyond the derivations in Refs. [12, 13]. With Eqs. (19) and (21), we start with the general formula for the probability of the n -photon process at $k = k_n$

$$|F_{n\pm}(\mathbf{k}, \omega)|_{k=k_n}^2 = \frac{\omega^2}{4\pi^2} \left| \int_{-\pi/\omega}^{\pi/\omega} dt \phi_{lm}(\mathbf{v}_{\pm}(t)) e^{iS_{\pm}(\mathbf{k}, t)} \right|_{k=k_n}^2, \quad (38)$$

where the action $S_{\pm}(\mathbf{k}, t)$ at $k = k_n$ is

$$S_{\pm}(\mathbf{k}, t)|_{k=k_n} = \mathbf{k}(\boldsymbol{\xi}_{\pm}(t) - \boldsymbol{\xi}_{\pm}(0))|_{k=k_n} + n\omega t. \quad (39)$$

It is also obtained by the well-known expression for the action

$$S_{\pm}(\mathbf{k}, t) = \frac{1}{2} \int_0^t \mathbf{v}_{\pm}(\tau)^2 d\tau + I_p t, \quad (40)$$

the conservation law (37), and the relation

$$\frac{1}{2} \int_0^t \mathbf{v}_{\pm}(\tau)^2 d\tau = \left(\frac{k^2}{2} + 2U_p \right) t + \mathbf{k}(\boldsymbol{\xi}_{\pm}(t) - \boldsymbol{\xi}_{\pm}(0)), \quad (41)$$

cf. Eq. (12). Using the saddle point method applied for $\omega \ll I_p$ and $\omega \ll U_p$, we obtain the simple expression for the probability of the n -photon process

$$|F_{n\pm}(\mathbf{k}, \omega)|_{k=k_n}^2 = \frac{\omega^2}{4\pi^2} \left| \phi_{lm}(\mathbf{v}_{\pm}(t_i)) e^{iS_{\pm}(\mathbf{k}, t_i)} \sqrt{\frac{2\pi}{S''_{\pm}(\mathbf{k}, t_i)}} \right|_{k=k_n}^2. \quad (42)$$

It means that the integral in Eq. (38) is accumulated mostly in the small region around the so-called (complex) ionization time t_i which is uniquely linked to \mathbf{k} and determined by the saddle point equation

$$\frac{\partial}{\partial t} S_{\pm}(\mathbf{k}, t) \Big|_{k=k_n, t=t_i} = \frac{\mathbf{v}_{\pm}(t_i)^2}{2} \Big|_{k=k_n} + I_p = \frac{\partial}{\partial t} \mathbf{k}\boldsymbol{\xi}_{\pm}(t) \Big|_{k=k_n, t=t_i} + n\omega = 0. \quad (43)$$

With

$$\mathbf{k}\xi_{\pm}(t)|_{k=k_n} = \frac{A_0\sqrt{k_n^2 - k_z^2}}{\omega} \cos(\omega t \mp \theta), \quad (44)$$

the saddle point equation (43) is rewritten as

$$\sin(\omega t_i \mp \theta) = \chi_n(k_z), \quad (45)$$

where

$$\chi_n(k_z) = \frac{n\omega}{A_0\sqrt{k_n^2 - k_z^2}} \geq \frac{n\omega}{A_0k_n} = \chi_n(k_z = 0) =: \chi_n. \quad (46)$$

Using Eqs. (31) and (33), the variable χ_n is reexpressed as

$$\chi_n = \sqrt{\frac{n^2\omega}{2A_0^2(n - n_0)}} = \sqrt{\frac{n^2(1 + \gamma^2)}{4n_0(n - n_0)}}, \quad (47)$$

where $\gamma = \sqrt{2I_p}/A_0 > 0$ is the Keldysh parameter [1] discriminating between adiabatic tunneling ($\gamma \ll 1$), non-adiabatic tunneling ($\gamma \sim 1$) [9], and multiphoton ionization ($\gamma \gg 1$). Eq. (47) is further rewritten as

$$\chi_n = \sqrt{\frac{1 + \gamma^2}{1 - \zeta^2}}, \quad (48)$$

where

$$\zeta = \frac{2n_0}{n} - 1 \in (-1, 1], \quad (49)$$

corresponding to the range $n \geq n_0$. In this range, χ_n is always larger than 1, thus $\chi_n(k_z) > 1$, cf. Eq. (46). Therefore, the ionization time t_i in Eq. (45) must be complex, i.e. $t_i = \text{Re } t_i + i \text{Im } t_i$, and we get two equations for $\text{Re } t_i$ and $\text{Im } t_i$,

$$\sin(\omega \text{Re } t_i \mp \theta) \cosh(\omega \text{Im } t_i) = \chi_n(k_z) \quad (50)$$

$$\cos(\omega \text{Re } t_i \mp \theta) \sinh(\omega \text{Im } t_i) = 0. \quad (51)$$

The corresponding solutions for $\text{Im } t_i \neq 0$ are

$$\omega \text{Re } t_i = \frac{\pi}{2} \pm \theta + 2\pi N, \quad (52)$$

$$\omega \text{Im } t_i = \text{arcosh } \chi_n(k_z), \quad (53)$$

where $N \in \mathbb{Z}$ is chosen such that $\omega \text{Re } t_i$ lies in the interval of a laser cycle, that is between $-\pi$ and π , cf. Eq. (38). The complex time t_i can be interpreted as the time of entering into the barrier, while its imaginary $\text{Im } t_i$ and real $\text{Re } t_i$ parts are the tunneling time and the time of exiting the barrier, respectively [14]. With Eqs. (44), (46), (52), (53), and $\sinh x = \sqrt{\cosh^2 x - 1}$, the corresponding action $S_{\pm}(\mathbf{k}, t_i)$ at $k = k_n$ (Eq. 39) is

$$S_{\pm}(\mathbf{k}, t_i)|_{k=k_n} = n \left(\frac{\pi}{2} \pm \theta + 2\pi N - \frac{\cos \theta}{\chi_n(k_z)} \right) + in \left(\text{arcosh } \chi_n(k_z) - \sqrt{1 - \frac{1}{\chi_n(k_z)^2}} \right). \quad (54)$$

Only its imaginary part

$$\text{Im } S(\mathbf{k}, t_i)|_{k=k_n} = n \left(\text{arcosh } \chi_n(k_z) - \sqrt{1 - \frac{1}{\chi_n(k_z)^2}} \right) \quad (55)$$

does not depend on the sense (\pm) of circular polarization, thus we can omit the index \pm of the imaginary part of the action. It means that the imaginary actions are equal for right and left circular polarizations. Using Eqs. (39), (44)–(46), the absolute value of the second derivative of the action $S''_{\pm}(\mathbf{k}, t_i)$ in Eq. (42) at $k = k_n$

$$\left| \frac{\partial^2}{\partial t^2} S(\mathbf{k}, t) \right|_{k=k_n, t=t_i} = n\omega^2 \sqrt{1 - \frac{1}{\chi_n(k_z)^2}} \quad (56)$$

is also independent of the sense (\pm) of circular polarization. Then, the expression for the probability of the n -photon process (42) is rewritten as

$$|F_{n\pm}(\mathbf{k}, \omega)|_{k=k_n}^2 = \frac{|\phi_{lm}(\mathbf{v}_{\pm}(t_i))|_{k=k_n}^2}{2\pi n \sqrt{1 - 1/\chi_n(k_z)^2}} e^{-2n(\text{arcosh } \chi_n(k_z) - \sqrt{1 - 1/\chi_n(k_z)^2})}. \quad (57)$$

Thus, the dependence of the ionization rate on the sense of circular polarization is only due to the prefactor

$$|\phi_{lm}(\mathbf{v}_{\pm}(t_i))|_{k=k_n}^2 = \frac{1}{4} |(\mathbf{v}_{\pm}(t_i)^2 + 2I_p)\tilde{\varphi}_{lm}(\mathbf{v}_{\pm}(t_i))|_{k=k_n}^2, \quad (58)$$

cf. Eq. (9). Using Eqs. (6), (52), and (53), the initial electron velocity

$$\mathbf{v}_{\pm}(t_i)|_{k=k_n} = v_{x\pm}(t_i)|_{k=k_n} \mathbf{e}_x + v_{y\pm}(t_i)|_{k=k_n} \mathbf{e}_y + k_z \mathbf{e}_z \quad (59)$$

with x - and y -components

$$v_{x\pm}(t_i)|_{k=k_n} = k_{\rho} \cos \theta - A_0(\chi_n(k_z) \cos \theta \mp i\sqrt{\chi_n(k_z)^2 - 1} \sin \theta) \quad (60)$$

$$v_{y\pm}(t_i)|_{k=k_n} = k_{\rho} \sin \theta - A_0(\chi_n(k_z) \sin \theta \pm i\sqrt{\chi_n(k_z)^2 - 1} \cos \theta) \quad (61)$$

specifies the required momentum of the initial wavefunction, i.e. $\tilde{\varphi}_{lm}(\mathbf{v}_{\pm}(t_i))$. The amount of this momentum depends on the orbital, in particular it is different for p_+ and p_- orbitals. Because of the saddle point equation (43), i.e. $\mathbf{v}_{\pm}(t_i)^2|_{k=k_n} + 2I_p = 0$, the initial wavefunction $\tilde{\varphi}_{lm}(\mathbf{v}_{\pm}(t_i))$ must have the pole at $\mathbf{v}_{\pm}(t_i)^2|_{k=k_n} = -2I_p = -\kappa^2$ that yields non-zero prefactor $|\phi_{lm}(\mathbf{v}_{\pm}(t_i))|_{k=k_n}^2$, cf. Eq. (58). For short-range potentials, it corresponds to the wavefunction in coordinate representation asymptotically far from the core [12], i.e.

$$\varphi_{lm}(\mathbf{r}) = C_{\kappa l} \kappa^{3/2} \frac{e^{-\kappa r}}{\kappa r} Y_{lm}(\theta_r, \phi_r), \quad (62)$$

with the constant $C_{\kappa l}$, depending on $\kappa = \sqrt{2I_p}$ and l as well as details of the potential near the core. Using spherical harmonics

$$Y_{lm}(\theta_r, \phi_r) = \sqrt{\frac{2l+1}{4\pi} \frac{(l-m)!}{(l+m)!}} P_l^m(\cos \theta_r) e^{im\phi_r}, \quad (63)$$

Fourier transformation (8), and

$$-i\mathbf{v}_{\pm}(t_i)\mathbf{r} = -iv_{\pm}(t_i)r(\sin \theta_{v\pm}(t_i) \sin \theta_r \cos(\phi_{v\pm}(t_i) - \phi_r) + \cos \theta_{v\pm}(t_i) \cos \theta_r) \quad (64)$$

in spherical coordinates, we evaluate two integrals over ϕ_r and θ_r with the help of the Bessel function and Ref. [29] to yield the intermediate result (see Appendix 4)

$$\tilde{\varphi}_{lm}(\mathbf{v}_{\pm}(t_i)) = C_{\kappa l} \sqrt{\frac{\kappa}{v_{\pm}(t_i)}} Y_{lm}(\theta_{v\pm}(t_i), \phi_{v\pm}(t_i)) e^{-il\pi/2} \int_0^{\infty} dr \sqrt{r} e^{-\kappa r} J_{l+1/2}(v_{\pm}(t_i)r). \quad (65)$$

Expanding the Bessel function in Taylor series and using the Gamma function $\Gamma(z)$, the integration over r is easily carried out. The resulting series is then compacted as the Gaussian

hypergeometric series (see Appendix 4)

$$\begin{aligned} \tilde{\varphi}_{lm}(\mathbf{v}_{\pm}(t_i)) &= \frac{C_{\kappa l}}{\sqrt{2\kappa^3}} \left(\frac{v_{\pm}(t_i)}{2\kappa} \right)^l Y_{lm}(\theta_{v_{\pm}(t_i)}, \phi_{v_{\pm}(t_i)}) e^{-il\pi/2} \\ &\quad \frac{\Gamma(l+2)}{\Gamma(l+3/2)} {}_2F_1 \left(\frac{l}{2} + 1, \frac{l}{2} + \frac{3}{2}; l + \frac{3}{2}; -\frac{v_{\pm}(t_i)^2}{\kappa^2} \right). \end{aligned} \quad (66)$$

The hypergeometric series does not converge at the saddle point $v_{\pm}(t_i)^2|_{k=k_n} = -\kappa^2$, thus this series has the pole as expected above. Multiplying Eq. (66) by $v_{\pm}(t_i)^2 + \kappa^2$ yields the series (see Appendix 4)

$$\begin{aligned} (v_{\pm}(t_i)^2 + \kappa^2) \tilde{\varphi}_{lm}(\mathbf{v}_{\pm}(t_i)) &= C_{\kappa l} \sqrt{\frac{2\kappa}{\pi}} \left(\frac{v_{\pm}(t_i)}{\kappa} \right)^l Y_{lm}(\theta_{v_{\pm}(t_i)}, \phi_{v_{\pm}(t_i)}) e^{-il\pi/2} \\ &\quad \frac{\sqrt{\pi}}{2^{l+1}} \frac{\Gamma(l+2)}{\Gamma(l+3/2)} {}_2F_1 \left(\frac{l}{2} + \frac{1}{2}, \frac{l}{2}; l + \frac{3}{2}; -\frac{v_{\pm}(t_i)^2}{\kappa^2} \right), \end{aligned} \quad (67)$$

which is convergent at the saddle point, i.e.

$$\frac{\sqrt{\pi}}{2^{l+1}} \frac{\Gamma(l+2)}{\Gamma(l+3/2)} {}_2F_1 \left(\frac{l}{2}, \frac{l}{2} + \frac{1}{2}; l + \frac{3}{2}; 1 \right) = 1. \quad (68)$$

Thus, the prefactor (58) is simplified as

$$|\phi_{lm}(\mathbf{v}_{\pm}(t_i))|_{k=k_n}^2 = \frac{|C_{\kappa l}|^2 \sqrt{2I_p}}{2\pi} |Y_{lm}(\theta_{v_{\pm}(t_i)}, \phi_{v_{\pm}(t_i)})|_{k=k_n}^2, \quad (69)$$

cf. Ref. [12]. With Eqs. (57) and (63), we finally obtain the general result for the probability of the n -photon process for all atomic orbitals

$$\begin{aligned} |F_{n\pm}(\mathbf{k}, \omega)|_{k=k_n}^2 &= \frac{|C_{\kappa l}|^2 \sqrt{2I_p} (2l+1)}{16\pi^3 n \sqrt{1-1/\chi_n(k_z)^2}} \frac{(l-|m|)!}{(l+|m|)!} \left| P_l^{|m|} \left(\frac{ik_z}{\sqrt{2I_p}} \right) \right|^2 |e^{im\phi_{v_{\pm}(t_i)}}|_{k=k_n}^2 \\ &\quad e^{-2n(\operatorname{arcosh} \chi_n(k_z) - \sqrt{1-1/\chi_n(k_z)^2})}, \end{aligned} \quad (70)$$

where $\cos \theta_{v_{\pm}(t_i)}|_{k=k_n} = v_z/v_{\pm}(t_i)|_{k=k_n} = \pm ik_z/\sqrt{2I_p}$ was used. The square of the associated Legendre polynomials in Eq. (70) are equal to 1 for s orbitals, $k_z^2/(2I_p)$ for p_0 orbitals, $(k_z^2 + 2I_p)/(2I_p)$ for p_{\pm} orbitals, and so on. The ionization rates for orbitals with $m = 0$ (e.g. s and p_0 orbitals) are independent of the sense of circular polarization. For $m \neq 0$ (e.g. p_{\pm} orbitals), they depend on the polarization sense, solely due to the factor $|e^{im\phi_{v_{\pm}(t_i)}}|_{k=k_n}^2$. For $m \neq 0$, this factor is not equal to unity, because the so-called tunneling momentum

angle $\phi_{v\pm}(t_i)$, which is related by

$$\cos \phi_{v\pm}(t_i) = \frac{v_{x\pm}(t_i)}{v_{\rho\pm}(t_i)} \quad (71)$$

$$\sin \phi_{v\pm}(t_i) = \frac{v_{y\pm}(t_i)}{v_{\rho\pm}(t_i)}, \quad (72)$$

is complex. With $v_{\rho\pm}(t_i)^2|_{k=k_n} = -(k_z^2 + 2I_p)$, $\gamma = \sqrt{2I_p}/A_0$, Eqs. (31), (46), (60), and (61), the factor $|e^{im\phi_{v\pm}(t_i)}|_{k=k_n}^2$ for $m = \pm 1$ is (see Appendix 5)

$$|e^{im\phi_{v\pm}(t_i)}|_{k=k_n}^2 = |\cos \phi_{v\pm}(t_i) + i \operatorname{sgn}(m) \sin \phi_{v\pm}(t_i)|_{k=k_n}^2 \quad (73)$$

$$= \frac{I_p \left[2\chi_n(k_z)^2 \left(1 \mp \operatorname{sgn}(m) \sqrt{1 - 1/\chi_n(k_z)^2} \right) - (1 + \gamma^2)n/n_0 \right]^2}{2\gamma^2\chi_n(k_z)^2 (k_z^2 + 2I_p)}. \quad (74)$$

Now, we can see that the ionization rates for a given circular polarization are different for orbitals with opposite quantum numbers $m = \pm 1$ (e.g. p_{\pm} orbitals). Because of the term $\mp \operatorname{sgn}(m)$ in Eq. (74), the ionization rate for the p_+ (or p_-) orbital and right circular polarization is the same as the ionization rate for the p_- (or p_+) orbital and left circular polarization, supporting the fundamental symmetry in electrodynamics.

E. Accurate formulas for the time-averaged ionization rates for s and p orbitals

Since the function $|F_{n\pm}(\mathbf{k}, \omega)|_{k=k_n}^2$ (Eq. (70)) depends only on k_z^2 , the two integrations over k_{ρ} and θ in the formula for the time-averaged ionization rate (Eqs. (35) and (36)) are easily carried out and the result is simplified to

$$w_{\pm}(\mathcal{E}, \omega) = 8\pi^2 \sum_{n \geq n_0}^{\infty} \int_0^{k_n} dk_z |F_{n\pm}(\mathbf{k}, \omega)|_{k=k_n}^2. \quad (75)$$

With Eqs. (70) and (74), the accurate formulas for the time-averaged ionization rates are

$$w^s(\mathcal{E}, \omega) = \frac{|C_{\kappa 0}|^2 \sqrt{2I_p}}{2\pi} \sum_{n \geq n_0}^{\infty} \frac{1}{n} \int_0^{k_n} dk_z \frac{e^{-2n(\operatorname{arcosh} \chi_n(k_z) - \sqrt{1 - 1/\chi_n(k_z)^2})}}{\sqrt{1 - 1/\chi_n(k_z)^2}} \quad (76)$$

for s orbitals,

$$w^{p_0}(\mathcal{E}, \omega) = \frac{3|C_{\kappa 1}|^2}{2\pi\sqrt{2I_p}} \sum_{n \geq n_0}^{\infty} \frac{1}{n} \int_0^{k_n} dk_z \frac{k_z^2 e^{-2n(\operatorname{arcosh} \chi_n(k_z) - \sqrt{1 - 1/\chi_n(k_z)^2})}}{\sqrt{1 - 1/\chi_n(k_z)^2}} \quad (77)$$

for p_0 orbitals, and

$$w_{\pm}^{p_{\pm}}(\mathcal{E}, \omega) = \frac{3|C_{\kappa 1}|^2 \sqrt{2I_p}}{16\pi\gamma^2} \sum_{n \geq n_0}^{\infty} \frac{1}{n} \int_0^{k_n} dk_z \frac{e^{-2n(\operatorname{arcosh} \chi_n(k_z) - \sqrt{1 - 1/\chi_n(k_z)^2})}}{\chi_n(k_z)^2 \sqrt{1 - 1/\chi_n(k_z)^2}} \quad (78)$$

$$\left[2\chi_n(k_z)^2 \left(1 \mp \operatorname{sgn}(m) \sqrt{1 - 1/\chi_n(k_z)^2} \right) - (1 + \gamma^2)n/n_0 \right]^2$$

for p_{\pm} orbitals.

F. Approximate formulas for the time-averaged ionization rates for s and p orbitals

In Eqs. (76)–(78), the exponential function has the maximum at $k_z = 0$, confirming our expectation that the electron leaves mostly in the polarization plane of the laser field, i.e. x/y -plane, and that the electron ionization along the propagation axis (z -axis) is suppressed. Therefore, we use Taylor series of the exponent at $k_z \approx 0$ up to second order, i.e.

$$\operatorname{arcosh} \chi_n(k_z) - \sqrt{1 - 1/\chi_n(k_z)^2} \approx \operatorname{arcosh} \chi_n - \sqrt{1 - 1/\chi_n^2} + \frac{1}{2} \sqrt{1 - 1/\chi_n^2} \left(\frac{k_z}{k_n} \right)^2. \quad (79)$$

The k_z -dependent prefactors in Eqs. (76)–(78) are then replaced by the non-vanishing lowest-order terms of the corresponding Taylor series at $k_z \approx 0$, i.e.

$$\frac{1}{\sqrt{1 - 1/\chi_n(k_z)^2}} \approx \frac{1}{\sqrt{1 - 1/\chi_n^2}} \quad (80)$$

for s orbitals,

$$\frac{k_z^2}{\sqrt{1 - 1/\chi_n(k_z)^2}} \approx \frac{k_z^2}{\sqrt{1 - 1/\chi_n^2}} \quad (81)$$

for p_0 orbitals, and

$$\frac{\left[2\chi_n(k_z)^2 \left(1 \mp \operatorname{sgn}(m) \sqrt{1 - 1/\chi_n(k_z)^2} \right) - (1 + \gamma^2)n/n_0 \right]^2}{\chi_n(k_z)^2 \sqrt{1 - 1/\chi_n(k_z)^2}} \quad (82)$$

$$\approx \frac{\left[2\chi_n^2 \left(1 \mp \operatorname{sgn}(m)\sqrt{1-1/\chi_n^2}\right) - (1+\gamma^2)n/n_0\right]^2}{\chi_n^2\sqrt{1-1/\chi_n^2}}$$

for p_{\pm} orbitals. For p_0 orbitals, the k_z -dependent prefactor in Eq. (81) has no zeroth-order term due to the existence of the factor k_z^2 . That means that the ionization rate for p_0 orbitals in the polarization plane is zero because of the destructive interference coming from two phase-opposite lobes. It also concludes that the approximation $k_z \approx 0$ for p_0 orbitals may be not very appropriate, i.e. the electron from the p_0 orbital will leave with non-zero final momentum component $k_z \neq 0$, i.e. parallel to the z -axis, due to its orbital shape. With the Taylor approximations (79)–(82), we evaluate the remaining integrals in Eqs. (76)–(78) over k_z as

$$\int_0^{k_n} dk_z e^{-a_n^2 \left(\frac{k_z}{k_n}\right)^2} = \frac{\sqrt{\pi} k_n \operatorname{erf}(a_n)}{2a_n} \quad (83)$$

and

$$\int_0^{k_n} dk_z k_z^2 e^{-a_n^2 \left(\frac{k_z}{k_n}\right)^2} = k_n^3 \left(\frac{\sqrt{\pi} \operatorname{erf}(a_n)}{4a_n^3} - \frac{e^{-a_n^2}}{2a_n^2} \right) \quad (84)$$

where $a_n = \sqrt{n} (1 - 1/\chi_n^2)^{1/4}$. For $\omega \ll I_p$, the minimal number of photons n_0 (Eq. (31)) must be very large. It follows that $n \geq n_0 \gg 1$, hence $\chi_n \gg 1$ (cf. Eqs. (48) and (49)) and $a_n \gg 1$. In the limit $a_n \rightarrow \infty$, the error function $\operatorname{erf}(a_n)$ and the exponential function $e^{-a_n^2}$ tend to unity and zero, respectively. For $\omega \ll I_p$, we use Eqs. (76)–(84) and Eqs. (31), (46), $A_0 = \sqrt{2I_p}/\gamma$, i.e. $k_n = n\omega\gamma/(\chi_n\sqrt{2I_p})$ and $\omega = I_p(1+\gamma^2)/(n_0\gamma^2)$, to obtain the approximate formuals for the time-averaged ionization rates

$$w^s(\mathcal{E}, \omega) = \frac{|C_{\kappa 0}|^2 I_p (1+\gamma^2)}{4\sqrt{\pi} n_0 \gamma} \sum_{n \geq n_0}^{\infty} \frac{e^{-2n(\operatorname{arcosh} \chi_n - \sqrt{1-1/\chi_n^2})}}{\sqrt{n} \chi_n (1-1/\chi_n^2)^{3/4}} \quad (85)$$

for s orbitals,

$$w^{p_0}(\mathcal{E}, \omega) = \frac{3|C_{\kappa 1}|^2 I_p (1+\gamma^2)^3}{32\sqrt{\pi} n_0^3 \gamma^3} \sum_{n \geq n_0}^{\infty} \frac{\sqrt{n} e^{-2n(\operatorname{arcosh} \chi_n - \sqrt{1-1/\chi_n^2})}}{\chi_n^3 (1-1/\chi_n^2)^{5/4}} \quad (86)$$

for p_0 orbitals, and

$$w_{\pm}^{p_{\pm}}(\mathcal{E}, \omega) = \frac{3|C_{\kappa 1}|^2 I_p (1 + \gamma^2)}{8\sqrt{\pi} n_0 \gamma^3} \sum_{n \geq n_0}^{\infty} \frac{\chi_n e^{-2n(\operatorname{arcosh} \chi_n - \sqrt{1 - 1/\chi_n^2})}}{\sqrt{n} (1 - 1/\chi_n^2)^{3/4}} \left[\sqrt{1 - 1/\chi_n^2} \mp (2n_0/n - 1) \operatorname{sgn}(m) \right]^2 \quad (87)$$

for p_{\pm} orbitals. These expressions Eqs. (85)–(87) depend on χ_n and n . If we use Eqs. (48) and (49) as well as $\operatorname{arcosh} \chi_n = \operatorname{artanh} \sqrt{1 - 1/\chi_n^2}$, then we obtain alternative expressions for the ionization rates depending on ζ , i.e.

$$w^s(\mathcal{E}, \omega) = \frac{|C_{\kappa 0}|^2 I_p}{4\sqrt{2\pi} n_0^{3/2}} \left(1 + \frac{1}{\gamma^2}\right)^{1/2} \sum_{n \geq n_0}^{\infty} (1 + \zeta) \sqrt{1 - \zeta} \left(\frac{1 + \gamma^2}{\zeta^2 + \gamma^2}\right)^{3/4} e^{-\frac{4n_0}{1+\zeta} \left(\operatorname{artanh} \sqrt{\frac{\zeta^2 + \gamma^2}{1 + \gamma^2}} - \sqrt{\frac{\zeta^2 + \gamma^2}{1 + \gamma^2}}\right)} \quad (88)$$

for s orbitals, where it coincides exactly with Eqs. (68) and (69) of Ref. [12],

$$w^{p_0}(\mathcal{E}, \omega) = \frac{3|C_{\kappa 1}|^2 I_p}{16\sqrt{2\pi} n_0^{5/2}} \left(1 + \frac{1}{\gamma^2}\right)^{3/2} \sum_{n \geq n_0}^{\infty} (1 - \zeta^2) \sqrt{1 - \zeta} \left(\frac{1 + \gamma^2}{\zeta^2 + \gamma^2}\right)^{5/4} e^{-\frac{4n_0}{1+\zeta} \left(\operatorname{artanh} \sqrt{\frac{\zeta^2 + \gamma^2}{1 + \gamma^2}} - \sqrt{\frac{\zeta^2 + \gamma^2}{1 + \gamma^2}}\right)} \quad (89)$$

for p_0 orbitals, and

$$w_{\pm}^{p_{\pm}}(\mathcal{E}, \omega) = \frac{3|C_{\kappa 1}|^2 I_p}{8\sqrt{2\pi} n_0^{3/2}} \left(1 + \frac{1}{\gamma^2}\right)^{3/2} \sum_{n \geq n_0}^{\infty} \left(\sqrt{\frac{\zeta^2 + \gamma^2}{1 + \gamma^2}} \mp \zeta \operatorname{sgn}(m) \right)^2 \frac{1}{\sqrt{1 - \zeta}} \left(\frac{1 + \gamma^2}{\zeta^2 + \gamma^2}\right)^{3/4} e^{-\frac{4n_0}{1+\zeta} \left(\operatorname{artanh} \sqrt{\frac{\zeta^2 + \gamma^2}{1 + \gamma^2}} - \sqrt{\frac{\zeta^2 + \gamma^2}{1 + \gamma^2}}\right)} \quad (90)$$

for p_{\pm} orbitals. Since $\left| \sqrt{(\zeta^2 + \gamma^2)/(1 + \gamma^2)} \right| \geq |\zeta|$, we recognize in Eq. (90) that the n -photon ionization rate is maximal for $\mp \operatorname{sgn}(m) = 1$ if $\zeta > 0$ and for $\pm \operatorname{sgn}(m) = 1$ if $\zeta < 0$. Therefore, for $\zeta > 0$ (low photon and kinetic energies) and e.g. for right circular polarization, the rate for p_- orbitals is larger than the one for p_+ orbitals. For $\zeta < 0$ (high photon and kinetic energies), however, the rate for p_+ orbitals is larger than the one for p_- orbitals. For $\zeta = 0$, corresponding to the photon energy $n\omega = 2n_0\omega = 4U_p + 2I_p$ and electron kinetic

energy $k_n^2/2 = (n - n_0)\omega = n_0\omega = 2U_p + I_p$, the ionization rates for both p_{\pm} orbitals are identical. By the way, we would like to stress that the ionization rate for p_0 orbitals (Eq. (89)) is very small compared to the rates for s and p_{\pm} orbitals, due to the ionization suppression in the polarization plane.

G. Simple formulas for the time-averaged ionization rates for s and p orbitals

To obtain the simple analytical expressions for the ionization rates, the summation over n -photon processes in Eqs. (88)–(90) can be replaced with integration over ζ , i.e.

$$\sum_{n \geq n_0}^{\infty} \approx \int_{n_0}^{\infty} dn = 2n_0 \int_{-1}^1 \frac{d\zeta}{(1 + \zeta)^2}. \quad (91)$$

For $\omega \ll I_p$, i.e. $n_0 \gg 1$, the saddle point method for integration over ζ is then applied, where the exponent in Eqs. (88)–(90)

$$S(\zeta, \gamma) = -\frac{4n_0}{1 + \zeta} \left(\operatorname{artanh} \sqrt{\frac{\zeta^2 + \gamma^2}{1 + \gamma^2}} - \sqrt{\frac{\zeta^2 + \gamma^2}{1 + \gamma^2}} \right) \quad (92)$$

has a unique maximum at $\zeta = \zeta_0(\gamma)$. This maximum is determined by the saddle point equation

$$\left. \frac{\partial}{\partial \zeta} S(\zeta, \gamma) \right|_{\zeta = \zeta_0} = 0, \quad (93)$$

that yields the transcendental equation for $\zeta_0(\gamma)$

$$\operatorname{artanh} \sqrt{\frac{\zeta_0^2 + \gamma^2}{1 + \gamma^2}} = \frac{1}{1 - \zeta_0} \sqrt{\frac{\zeta_0^2 + \gamma^2}{1 + \gamma^2}}, \quad (94)$$

or equivalently

$$\operatorname{artanh} \sqrt{1 - 1/\chi_{n_{\max}}^2} = \frac{1}{2} \frac{n_{\max}}{n_{\max} - n_0} \sqrt{1 - 1/\chi_{n_{\max}}^2}, \quad (95)$$

where $\chi_{n_{\max}} = \sqrt{(1 + \gamma^2)/(1 - \zeta_0^2)}$ (cf. Eq. (48)) and $n_{\max} = 2n_0/(1 + \zeta_0)$ is the number of photons for which the n -photon ionization rate is maximal, corresponding to the electron kinetic energy $k_{n_{\max}}^2/2 = (n_{\max} - n_0)\omega = (2U_p + I_p)(1 - \zeta_0)/(1 + \zeta_0)$. Since the solution of

Eq. (94) is in the positive range $\zeta_0(\gamma) \in [0, 1]$, the maximum of the (n_{\max} -photon) ionization rate for right (left) circular polarization is dominated by the electron ionization from the p_- (p_+) orbital. In the adiabatic limit ($\gamma \ll 1$), the solution is approximated as $\zeta_0(\gamma) \approx \gamma^2/3$ (see Ref. [12] and Appendix 6), corresponding to the electron kinetic energy $k_{n_{\max}}^2/2 \approx (2U_p + I_p)(1 - 2\gamma^2/3) \approx 2U_p + I_p/3$, whereas in the non-adiabatic limit ($\gamma \gg 1$), it yields $\zeta_0(\gamma) \approx 1 - 1/\ln \gamma$, see Ref. [12]. The exponent (Eq. (92)) at the saddle point $\zeta_0(\gamma)$ is

$$S(\zeta_0, \gamma) = -\frac{2\mathcal{E}_0}{3\mathcal{E}} g(\gamma), \quad (96)$$

where $\mathcal{E}_0 = (2I_p)^{3/2}$ and

$$g(\gamma) = \frac{3\zeta_0}{\gamma^2(1 - \zeta_0^2)} \sqrt{(1 + \gamma^2)(\zeta_0^2/\gamma^2 + 1)}, \quad (97)$$

and it does not depend on orbitals. We also need the second derivative of the exponent $S''(\zeta_0, \gamma)$, i.e.

$$\left. \frac{\partial^2}{\partial \zeta^2} S(\zeta, \gamma) \right|_{\zeta=\zeta_0} = -\frac{4n_0(2\zeta_0^2 + \zeta_0^2\gamma^2 + \gamma^2)}{(1 + \zeta_0)^3(1 - \zeta_0)^2(\zeta_0^2 + \gamma^2)} \sqrt{\frac{\zeta_0^2 + \gamma^2}{1 + \gamma^2}}, \quad (98)$$

to apply the saddle point method according to

$$\int_{-1}^1 d\zeta f(\zeta) e^{S(\zeta, \gamma)} = f(\zeta_0) e^{S(\zeta_0, \gamma)} \sqrt{\frac{2\pi}{-S''(\zeta_0, \gamma)}}. \quad (99)$$

Therefore, with these equations and Eqs. (88)–(90), we obtain the compact expressions for the time-averaged ionization rates

$$w^s(\mathcal{E}, \omega) = |C_{\kappa 0}|^2 I_p \frac{\mathcal{E}}{2\mathcal{E}_0} h^s(\gamma) e^{-\frac{2\mathcal{E}_0}{3\mathcal{E}} g(\gamma)} \quad (100)$$

for s orbitals,

$$w^{p_0}(\mathcal{E}, \omega) = |C_{\kappa 1}|^2 I_p \frac{\mathcal{E}}{2\mathcal{E}_0} h^{p_0}(\gamma) e^{-\frac{2\mathcal{E}_0}{3\mathcal{E}} g(\gamma)} \quad (101)$$

for p_0 orbitals, and

$$w_{\pm}^{p_{\pm}}(\mathcal{E}, \omega) = |C_{\kappa 1}|^2 I_p \frac{\mathcal{E}}{2\mathcal{E}_0} h_{\pm}^{p_{\pm}}(\gamma) e^{-\frac{2\mathcal{E}_0}{3\mathcal{E}} g(\gamma)} \quad (102)$$

for p_{\pm} orbitals, where

$$h^s(\gamma) = (1 - \zeta_0) \sqrt{\frac{(1 + \gamma^2)(1 - \zeta_0^2)}{(\zeta_0^2/\gamma^2 + 1)(2\zeta_0^2/\gamma^2 + \zeta_0^2 + 1)}} \quad (103)$$

$$h^{p_0}(\gamma) = h^s(\gamma) \frac{3\mathcal{E}}{2\mathcal{E}_0} (1 - \zeta_0) \sqrt{\frac{1 + \gamma^2}{\zeta_0^2/\gamma^2 + 1}} \quad (104)$$

$$h_{\pm}^{p_{\pm}}(\gamma) = h^s(\gamma) \frac{3(1 + \gamma^2)}{2(1 - \zeta_0^2)} \left(\sqrt{\frac{\zeta_0^2/\gamma^2 + 1}{1 + \gamma^2}} \mp \frac{\zeta_0}{\gamma} \operatorname{sgn}(m) \right)^2. \quad (105)$$

For s orbitals, Eqs. (97) and (103) coincide exactly with Eqs. (73) and (74) of Ref. [12]. In the adiabatic limit $\gamma \ll 1$, i.e. $\zeta_0(\gamma \ll 1) \approx \gamma^2/3(1 - 28\gamma^2/45)$ (see Ref. [12] and Appendix 6), the exponent and prefactors in Taylor series up to second order in γ are

$$g(\gamma \ll 1) \approx 1 - \gamma^2/15 \quad (106)$$

$$h^s(\gamma \ll 1) \approx 1 \quad (107)$$

$$h^{p_0}(\gamma \ll 1) \approx \frac{3\mathcal{E}}{2\mathcal{E}_0} \left(1 + \frac{\gamma^2}{9} \right) \quad (108)$$

$$h_{\pm}^{p_{\pm}}(\gamma \ll 1) \approx \frac{3}{2} \mp \gamma \operatorname{sgn}(m) + \frac{\gamma^2}{3}. \quad (109)$$

Therefore, the ratio of the ionization rates for p_{\pm} orbitals

$$\frac{w_{\pm}^{p_{-}}(\mathcal{E}, \omega)}{w_{\pm}^{p_{+}}(\mathcal{E}, \omega)} \approx 1 \pm \frac{4\gamma}{3} + \frac{8\gamma^2}{9} \quad (\gamma \ll 1) \quad (110)$$

is always larger than 1 for right circular polarization and smaller than 1 for left circular polarization. That means, for e.g. right circular polarization, the ionization from p_{-} orbitals is more preferred than the ionization from p_{+} orbitals. In the adiabatic case $\gamma = 0$, i.e. the tunneling is much faster than the rotation of the laser field, the ionization rates for p_{\pm} orbitals are equal as expected. In the non-adiabatic limit $\gamma \gg 1$, i.e. $\zeta_0(\gamma) \approx 1 - 1/\ln \gamma$, the exponent and prefactors are approximated as

$$g(\gamma \gg 1) \approx \frac{3 \ln \gamma}{2\gamma} \quad (111)$$

$$h^s(\gamma \gg 1) \approx \frac{\gamma}{(\ln \gamma)^{3/2}} \quad (112)$$

$$h^{p_0}(\gamma \gg 1) \approx \frac{3\mathcal{E}}{2\mathcal{E}_0} \frac{\gamma^2}{(\ln \gamma)^{5/2}} \quad (113)$$

$$h_{\pm}^{p_{\pm}}(\gamma \gg 1) = \frac{3}{4} \frac{\gamma}{(\ln \gamma)^{1/2}} \left[1 \mp \left(1 - \frac{1}{\ln \gamma} \right) \text{sgn}(m) \right]^2.$$

Thus, the ratio of the ionization rates for p_{\pm} orbitals is

$$\frac{w_{\pm}^{p_{-}}(\mathcal{E}, \omega)}{w_{\pm}^{p_{+}}(\mathcal{E}, \omega)} \approx (2 \ln \gamma)^{\pm 2} \quad (\gamma \gg 1), \quad (114)$$

i.e. for right circular polarization, the ionization rate for p_{-} orbitals is much larger than the one for p_{+} orbitals.

III. RESULTS AND DISCUSSION

For application, we use Kr atom in the ground state with ionization potential $I_p = 0.5$ a.u. An infrared circularly polarized strong laser field with typical experimental parameters of the laser frequency $\omega = 0.057$ a.u. (800 nm) and the laser amplitude $\mathcal{E} = 0.06$ a.u. ($I = 2.5 \cdot 10^{14}$ W/cm²) ionizes an electron from the $4p$ valence orbital of the Kr atom. In this experimental example, the Keldysh parameter is $\gamma = \omega/\mathcal{E}\sqrt{2I_p} = 0.95$, thus an $4p$ electron tunnels the ionization barrier non-adiabatically with respect to the rotation of the electric field. Although this is indeed non-adiabatic tunneling, many previous theoretical works are based on adiabatic approximation that cannot predict the difference of the ionization rates for p_{+} and p_{-} orbitals in circularly polarized laser fields. With our analytical formulas derived in Section II, which are beyond the original work [12, 13], we present the results in Figs. 1–3 and show that the ionization rates for p_{+} and p_{-} valence orbitals are indeed very different, supporting our physical interpretation in the previous work [10]. We also show the results for the ionization rates for p_0 orbitals in Figs. 1–3. Although the results for the ionization rates for s orbitals have nothing to do with the ionization of the Kr atom, we would like to include these results in Figs. 1–3 as well, but these results cannot be compared with the ones for p orbitals due to the generally different factors $C_{\kappa l}$ for s and p orbitals depending on the model system. However, in all calculations, we have used $C_{\kappa l} = 1$ for simplicity.

In Fig. 1, the results for ionization rates depending on the laser frequency up to $\omega = 0.12$ a.u. for laser amplitude $\mathcal{E} = 0.06$ a.u. are shown. The orange, green, blue, and red curves correspond to the rates for s , p_0 , p_{+} , and p_{-} orbitals, and the associated solid, dashed, and

dotted curves correspond to the accurate (Eqs. (76)–(78)), approximate (Eqs. (88)–(90)), and simple (Eqs. (100)–(102)) results, respectively. For s orbitals, the approximate and simple results coincide with each other very well within graphical resolution. The accurate results for s orbitals are a little separated from approximate and simple results, mainly due to the integral approximations (83) and (84) for $\omega \ll I_p$. For p_0 orbitals, the ionization rates are very small compared to the ones for p_{\pm} orbitals, supporting our thoughts in Section II.E, i.e. the destructive interference coming from two phase-opposite lobes of the p_0 orbital causes ionization suppression in the polarization plane perpendicular to the orbital nodal axis. Again by more precise inspection, the approximate and simple results are similar while the accurate results are a little separated from the approximate and simple results, again mainly due to approximations (83) and (84) for $\omega \ll I_p$. While the ionization rates for s and p_0 orbitals do not depend on the sense of circular polarization, the rates for p_+ and p_- orbitals do. For right circular polarization, the rates for p_- orbitals are larger than the ones for p_+ orbitals by the ratio up to 6 for large frequencies. For left circular polarization, the physical behaviour is reversed according to the fundamental symmetry in electrodynamics, i.e. the ionization rates for p_{\pm} orbitals and left circular polarization are equal to the ones for p_{\mp} orbitals and right circular polarization. In the adiabatic limit $\gamma = \omega = 0$, the rates for both p_{\pm} orbitals are exactly equal as already predicted in many previous theoretical works based on adiabatic approximation. For p_{\pm} orbitals there are some (but not large) deviations between accurate, approximate, and simple results in particular for large frequencies or equivalently for large γ , but in the adiabatic ($\gamma \ll 1$) and non-adiabatic ($\gamma \sim 1$) tunneling regimes, these three results for p_+ and for p_- converge well. The small differences for large frequencies are not only due to the saddle point method (which is only applicable for low frequencies) but also due to the integral approximations (83) and (84) for $\omega \ll I_p$.

Fig. 2 shows the monotonically increased ionization rates for s and p orbitals versus laser intensity $I = c^2 \varepsilon_0^2 \mathcal{E}^2$ in the range from $2 \cdot 10^{13}$ W/cm² to $2 \cdot 10^{14}$ W/cm² (corresponding to the laser amplitude \mathcal{E} in the range from 0.0169 a.u. to 0.0534 a.u.) for laser frequency $\omega = 0.057$ a.u. (800 nm) in logarithmic scale. In this figure, the accurate, approximate, and simple results coincide within graphical resolution. As already explained above, the rates for p_0 orbitals are small compared to the rates for p_{\pm} orbitals. For right circular polarization, the rates for p_- orbitals are larger than the ones for p_+ orbitals. The corresponding ratio is large (small) for low (high) laser intensities or equivalently for large (small) γ .

Fig. 3 shows the photoelectron spectra for s and p orbitals, right circular polarization, laser amplitude $\mathcal{E} = 0.06$ a.u., and laser frequency $\omega = 0.057$ a.u. (800 nm). The curves are calculated using time-averaged n -photon ionization rates $w_{n+}(\mathcal{E}, \omega)$ (Eq. (36)) versus final electronic kinetic energy at the detector $k_n^2/2$ (Eq. (37)). Since there are no sums in simple results (Eqs. (100)–(102)), only the corresponding accurate (solid) and approximate (dashed) spectra (cf. Eqs. (88)–(90) and Eqs. (100)–(102)) are presented in this figure, as well as the spectra for total p orbitals according to $w_{n+}^p(\mathcal{E}, \omega) = w_{n+}^{p_0}(\mathcal{E}, \omega) + w_{n+}^{p_+}(\mathcal{E}, \omega) + w_{n+}^{p_-}(\mathcal{E}, \omega)$. In fact, the spectra are different for electrons coming from different orbitals. For right circular polarization, the ionization from p_- orbitals is dominant, but there is a unique kinetic energy for which the n -photon ionization rates for p_+ and p_- orbitals are equal. This is the final kinetic energy $2U_p + I_p \approx 1.05$ a.u. for the approximate results. For the accurate results, the intersection of the spectra for p_+ and p_- orbitals lies at the energy a little more than $2U_p + I_p$. Below (above) this unique electronic final kinetic energy, the ionization rates for p_- orbitals are larger (smaller) than the ones for p_+ orbitals. Therefore, the final kinetic energy indicates the strength and the direction of the ring current [26, 27] generated in the ion, measured in correlation with the electron. Low energy electrons correlate to the ions with positive ring currents, while higher energy electrons correlate to the ions with negative ring currents. Furthermore, the locations of the maxima for s , p_0 , and total p orbitals are similar, whereas the ones for p_- orbitals are shifted to lower energy and the ones for p_+ orbitals are shifted to higher energy. The reason is that the counter-clockwise (“positive”, right) sense of circular polarization drives the electron from p_- and p_+ orbitals with clockwise (“negative”) and counter-clockwise (“positive”) azimuthal velocities, yielding smaller and larger kinetic energies, respectively. In the adiabatic limit $\gamma \ll 1$, all photoelectron spectra have its maxima at $2U_p \approx 0.55$ a.u. and in this case the spectra for p_+ and p_- orbitals are identical.

IV. CONCLUSIONS

We have validated the approximations used in our previous publication to derive simple formulas for ionization from different sub-states of the p orbitals. We extended the PPT theory to strong field non-adiabatic ionization for valence p orbitals and we derived the corresponding ionization rates in full analytical form. Due to the existence of the complex-valued tunneling angle in the prefactor of the ionization rate, the rates are different for

degenerate p_+ and p_- orbitals and depend on the sense of rotation of the circularly polarized laser fields. Strong field ionization preferentially removes a counter-rotating electron. As expected ionization rates for degenerate p_+ and p_- orbitals are significantly larger than the rates for p_0 orbitals due its orbital symmetry. We have also demonstrated that ionization rates and electron spectra obtained in this approach are gauge-invariant, unlike the results of the strong field approximation.

An important extension of this work is the consideration of the electron spin [30] to describe electronic ring currents in the ion, which couple electronic spin and orbital degree of freedom. Other possible extensions of this work include the theory of the non-adiabatic ionization for p orbitals in circularly or elliptically polarized laser fields and static magnetic fields, see also works for s orbitals [31, 32].

ACKNOWLEDGMENTS

We gratefully acknowledge stimulating discussions with E. Goulielmakis, M. Ivanov, U. Keller, J. Manz, and A. Wirth. The work was supported by the DFG Grant No. Sm 292/2-1.

APPENDIX 1

Here, we evaluate the ϕ -integral in Eq. (26)

$$I_1 = \int_0^{2\pi} d\phi e^{i\rho((k_{2x}-k_{1x})\cos\phi+(k_{2y}-k_{1y})\sin\phi)} (f_{\pm}(k_{1\rho}, \theta_1, \phi, t) + f_{\pm}(k_{2\rho}, \theta_2, \phi, t)). \quad (115)$$

Using the expression for the function $f_{\pm}(k_{\rho}, \theta, \phi, t)$ (Eq. (13)) and the Euler's formula, the prefactor of the integrand in Eq. (115) is rewritten as

$$\begin{aligned} & f_{\pm}(k_{1\rho}, \theta_1, \phi, t) + f_{\pm}(k_{2\rho}, \theta_2, \phi, t) \\ &= \frac{1}{2} (k_{1\rho}e^{i\theta_1} + k_{2\rho}e^{i\theta_2} \pm 2iA_0e^{\pm i\omega t}) e^{-i\phi} + \frac{1}{2} (k_{1\rho}e^{-i\theta_1} + k_{2\rho}e^{-i\theta_2} \mp 2iA_0e^{\mp i\omega t}) e^{i\phi}, \end{aligned} \quad (116)$$

hence

$$\begin{aligned} I_1 &= \frac{1}{2} (k_{1\rho}e^{i\theta_1} + k_{2\rho}e^{i\theta_2} \pm 2iA_0e^{\pm i\omega t}) \int_0^{2\pi} d\phi e^{-i\phi} e^{i\rho((k_{2x}-k_{1x})\cos\phi+(k_{2y}-k_{1y})\sin\phi)} \\ &\quad + \frac{1}{2} (k_{1\rho}e^{-i\theta_1} + k_{2\rho}e^{-i\theta_2} \mp 2iA_0e^{\mp i\omega t}) \int_0^{2\pi} d\phi e^{i\phi} e^{i\rho((k_{2x}-k_{1x})\cos\phi+(k_{2y}-k_{1y})\sin\phi)}. \end{aligned} \quad (117)$$

We use the substitution $|\mathbf{k}_{2\parallel} - \mathbf{k}_{1\parallel}| \sin\phi' = (k_{2x} - k_{1x})\cos\phi + (k_{2y} - k_{1y})\sin\phi$, which is satisfied by the relations ($\sin\phi = \sqrt{1 - \cos^2\phi}$)

$$\cos\phi = \frac{(k_{2x} - k_{1x})\sin\phi' + (k_{2y} - k_{1y})\cos\phi'}{|\mathbf{k}_{2\parallel} - \mathbf{k}_{1\parallel}|} \quad (118)$$

$$\sin\phi = \frac{(k_{2y} - k_{1y})\sin\phi' - (k_{2x} - k_{1x})\cos\phi'}{|\mathbf{k}_{2\parallel} - \mathbf{k}_{1\parallel}|}. \quad (119)$$

With Euler's formula, we obtain

$$e^{\pm i\phi} = \frac{\mp i(k_{2x} - k_{1x}) + (k_{2y} - k_{1y})}{|\mathbf{k}_{2\parallel} - \mathbf{k}_{1\parallel}|} e^{\pm i\phi'} \quad (120)$$

$$= \mp i \frac{k_{2\rho}e^{\pm i\theta_2} - k_{1\rho}e^{\pm i\theta_1}}{|\mathbf{k}_{2\parallel} - \mathbf{k}_{1\parallel}|} e^{\pm i\phi'} \quad (121)$$

and $d\phi = d\phi'$. The integral I_1 is then reexpressed as

$$\begin{aligned} I_1 &= \frac{i}{2} (k_{1\rho}e^{i\theta_1} + k_{2\rho}e^{i\theta_2} \pm 2iA_0e^{\pm i\omega t}) \frac{k_{2\rho}e^{-i\theta_2} - k_{1\rho}e^{-i\theta_1}}{|\mathbf{k}_{2\parallel} - \mathbf{k}_{1\parallel}|} \int_0^{2\pi} d\phi' e^{-i\phi'} e^{i\rho|\mathbf{k}_{2\parallel} - \mathbf{k}_{1\parallel}| \sin\phi'} \\ &\quad - \frac{i}{2} (k_{1\rho}e^{-i\theta_1} + k_{2\rho}e^{-i\theta_2} \mp 2iA_0e^{\mp i\omega t}) \frac{k_{2\rho}e^{i\theta_2} - k_{1\rho}e^{i\theta_1}}{|\mathbf{k}_{2\parallel} - \mathbf{k}_{1\parallel}|} \int_0^{2\pi} d\phi' e^{i\phi'} e^{i\rho|\mathbf{k}_{2\parallel} - \mathbf{k}_{1\parallel}| \sin\phi'}. \end{aligned} \quad (122)$$

With the definition of the Bessel function of the first kind

$$J_n(x) = \frac{1}{2\pi} \int_0^{2\pi} d\phi e^{-in\phi} e^{ix \sin \phi} = \frac{(-1)^n}{2\pi} \int_0^{2\pi} d\phi e^{in\phi} e^{ix \sin \phi}, \quad (123)$$

the integral is evaluated as

$$I_1 = \pi i \left[(k_{1\rho} e^{i\theta_1} + k_{2\rho} e^{i\theta_2} \pm 2iA_0 e^{\pm i\omega t}) (k_{2\rho} e^{-i\theta_2} - k_{1\rho} e^{-i\theta_1}) \right. \\ \left. + (k_{1\rho} e^{-i\theta_1} + k_{2\rho} e^{-i\theta_2} \mp 2iA_0 e^{\mp i\omega t}) (k_{2\rho} e^{i\theta_2} - k_{1\rho} e^{i\theta_1}) \right] \frac{J_1(\rho|\mathbf{k}_{2\parallel} - \mathbf{k}_{1\parallel}|)}{|\mathbf{k}_{2\parallel} - \mathbf{k}_{1\parallel}|}, \quad (124)$$

which is further simplified to

$$I_1 = 2\pi i (k_{2\rho}^2 - k_{1\rho}^2 - 2k_{2\rho}A_0 \sin(\omega t \mp \theta_2) + 2k_{1\rho}A_0 \sin(\omega t \mp \theta_1)) \frac{J_1(\rho|\mathbf{k}_{2\parallel} - \mathbf{k}_{1\parallel}|)}{|\mathbf{k}_{2\parallel} - \mathbf{k}_{1\parallel}|}, \quad (125)$$

cf. Eq. (26).

APPENDIX 2

In this appendix we prove the relation (Eq. 28)

$$\lim_{\rho \rightarrow \infty} \int d\mathbf{k}_{\parallel} g(\mathbf{k}_{\parallel}) \frac{\rho J_1(\rho k_{\parallel})}{k_{\parallel}} = 2\pi \int d\mathbf{k}_{\parallel} g(\mathbf{k}_{\parallel}) \delta(\mathbf{k}_{\parallel}) \quad (126)$$

with the arbitrary function $g(\mathbf{k}_{\parallel})$ and $k_{\parallel} = k_{\rho}$ as

$$\lim_{\rho \rightarrow \infty} \int d\mathbf{k}_{\parallel} g(\mathbf{k}_{\parallel}) \frac{\rho J_1(\rho k_{\parallel})}{k_{\parallel}} = \lim_{\rho \rightarrow \infty} \int_0^{2\pi} d\theta \int_0^{\infty} dk_{\rho} g(k_{\rho} \cos \theta \mathbf{e}_x + k_{\rho} \sin \theta \mathbf{e}_y) \rho J_1(\rho k_{\rho}) \quad (127)$$

$$= \lim_{\rho \rightarrow \infty} \int_0^{2\pi} d\theta \int_0^{\infty} dx g\left(\frac{x}{\rho} \cos \theta \mathbf{e}_x + \frac{x}{\rho} \sin \theta \mathbf{e}_y\right) J_1(x) \quad (128)$$

$$= \int_0^{2\pi} d\theta \int_0^{\infty} dx g(\mathbf{0}) J_1(x) \quad (129)$$

$$= 2\pi g(\mathbf{0}) \int_0^{\infty} dx J_1(x) \quad (130)$$

$$= 2\pi g(\mathbf{0}) \quad (131)$$

$$= 2\pi \int d\mathbf{k}_{\parallel} g(\mathbf{k}_{\parallel}) \delta(\mathbf{k}_{\parallel}). \quad (132)$$

APPENDIX 3

In this section we will evaluate k_+ - and k_- -integrals in Eq. (29). First with Eq. (31), we rearrange the denominator of the k_+ -integrand in Eq. (29) as

$$\begin{aligned} & \left[\frac{1}{4}(k_+ - k_-)^2 + k_y^2 + k_z^2 + A_0^2 + 2I_p - 2n_1\omega + i\delta \right] \\ & \left[\frac{1}{4}(k_+ + k_-)^2 + k_y^2 + k_z^2 + A_0^2 + 2I_p - 2n_2\omega - i\delta \right] \\ & = \frac{1}{16} [(k_+ - k_-)^2 - 4K_1 + 4i\delta] [(k_+ + k_-)^2 - 4K_2 - 4i\delta], \end{aligned} \quad (133)$$

where $K_{1,2} = 2(n_{1,2} - n_0)\omega - k_y^2 - k_z^2$. It has four zeros $k_+ = k_{1\pm}, k_{2\pm}$, i.e.

$$k_{1\pm} = \pm 2\sqrt{K_1 - i\delta} + k_- \quad (134)$$

$$k_{2\pm} = \pm 2\sqrt{K_2 + i\delta} - k_-. \quad (135)$$

Using Taylor series $\lim_{\delta \rightarrow 0} \sqrt{K \pm i\delta} = \lim_{\delta \rightarrow 0} \left(\sqrt{K} \pm i\delta/(2\sqrt{K}) \right)$, the zeros are rewritten as

$$k_{1\pm} = \pm 2\sqrt{K_1} + k_- \mp \frac{i\delta}{\sqrt{K_1}} \quad (136)$$

$$k_{2\pm} = \pm 2\sqrt{K_2} - k_- \pm \frac{i\delta}{\sqrt{K_2}}. \quad (137)$$

Thus, the k_+ -integrand in Eq. (29) is

$$\tilde{h}_{\pm}(k_+) = \left[\frac{1}{4}(k_+ - k_-)^2 + k_y^2 + k_z^2 + A_0^2 + 2I_p - 2n_1\omega + i\delta \right]^{-1} \quad (138)$$

$$\begin{aligned} & \left[\frac{1}{4}(k_+ + k_-)^2 + k_y^2 + k_z^2 + A_0^2 + 2I_p - 2n_2\omega - i\delta \right]^{-1} h_{\pm}(k_+) \\ & = \frac{16h_{\pm}(k_+)}{(k_+ - k_{1+})(k_+ - k_{1-})(k_+ - k_{2+})(k_+ - k_{2-})}. \end{aligned} \quad (139)$$

The corresponding integral is then evaluated using the residue method as

$$\int_{-\infty}^{\infty} dk_+ \tilde{h}_{\pm}(k_+) = 2\pi i \sum_{k=k_{1\pm}, k_{2\pm}} \Theta(\text{Im } k) \text{Res } \tilde{h}_{\pm}(k), \quad (140)$$

where the residues are calculated as

$$\text{Res } \tilde{h}_{\pm}(k) = \lim_{k_+ \rightarrow k} (k_+ - k) \tilde{h}_{\pm}(k_+), \quad (141)$$

in particular

$$\text{Res } \tilde{h}_{\pm}(k_{1+}) = \frac{8h_{\pm}(k_{1+})}{\left(2\sqrt{K_1} - \frac{i\delta}{\sqrt{K_1}}\right)} \left(2\sqrt{K_1} - 2\sqrt{K_2} + 2k_- - \frac{i\delta}{\sqrt{K_1}} - \frac{i\delta}{\sqrt{K_2}}\right)^{-1} \quad (142)$$

$$\text{Res } \tilde{h}_{\pm}(k_{1-}) = -\frac{8h_{\pm}(k_{1-})}{\left(2\sqrt{K_1} - \frac{i\delta}{\sqrt{K_1}}\right)} \left(2\sqrt{K_1} + 2\sqrt{K_2} + 2k_- - \frac{i\delta}{\sqrt{K_1}} + \frac{i\delta}{\sqrt{K_2}}\right)^{-1} \quad (143)$$

$$\text{Res } \tilde{h}_{\pm}(k_{2+}) = -\frac{8h_{\pm}(k_{2+})}{\left(2\sqrt{K_2} + \frac{i\delta}{\sqrt{K_2}}\right)} \left(2\sqrt{K_1} - 2\sqrt{K_2} + 2k_- - \frac{i\delta}{\sqrt{K_1}} - \frac{i\delta}{\sqrt{K_2}}\right)^{-1} \quad (144)$$

$$\text{Res } \tilde{h}_{\pm}(k_{2-}) = \frac{8h_{\pm}(k_{2-})}{\left(2\sqrt{K_2} + \frac{i\delta}{\sqrt{K_2}}\right)} \left(2\sqrt{K_1} + 2\sqrt{K_2} + 2k_- - \frac{i\delta}{\sqrt{K_1}} + \frac{i\delta}{\sqrt{K_2}}\right)^{-1} \quad (145)$$

$$\left(2\sqrt{K_1} - 2\sqrt{K_2} - 2k_- - \frac{i\delta}{\sqrt{K_1}} - \frac{i\delta}{\sqrt{K_2}}\right)^{-1}.$$

For $\delta = 0$, $k_- = 0$ and $0 \neq n_1 \neq n_2 \neq 0$, i.e. $0 \neq K_1 \neq K_2 \neq 0$, all four residues (142)–(145) are finite. Therefore, the k_- -integral in Eq. (29) would be zero due to the existence of the factor k_- in the integrand. Thus, the condition $n = n_1 = n_2$, i.e. $K = K_1 = K_2$, must be satisfied and the residues (142)–(145) are simplified to

$$\text{Res } \tilde{h}_{\pm}(k_{1+}) = \frac{2h_{\pm}(k_{1+})}{\left(2\sqrt{K} - \frac{i\delta}{\sqrt{K}}\right) \left(2\sqrt{K} + k_-\right) \left(k_- - \frac{i\delta}{\sqrt{K}}\right)} \quad (146)$$

$$\text{Res } \tilde{h}_{\pm}(k_{1-}) = \frac{2h_{\pm}(k_{1-})}{\left(2\sqrt{K} - \frac{i\delta}{\sqrt{K}}\right) \left(2\sqrt{K} - k_-\right) \left(k_- + \frac{i\delta}{\sqrt{K}}\right)} \quad (147)$$

$$\text{Res } \tilde{h}_{\pm}(k_{2+}) = -\frac{2h_{\pm}(k_{2+})}{\left(2\sqrt{K} + \frac{i\delta}{\sqrt{K}}\right) \left(2\sqrt{K} - k_-\right) \left(k_- - \frac{i\delta}{\sqrt{K}}\right)} \quad (148)$$

$$\text{Res } \tilde{h}_{\pm}(k_{2-}) = -\frac{2h_{\pm}(k_{2-})}{\left(2\sqrt{K} + \frac{i\delta}{\sqrt{K}}\right) \left(2\sqrt{K} + k_{-}\right) \left(k_{-} + \frac{i\delta}{\sqrt{K}}\right)}. \quad (149)$$

For $K < 0$, only two poles k_{1+} and k_{2+} have positive imaginary parts, therefore only two corresponding residues contribute to the k_{+} -integral (140), but in the limit $\delta = 0$ and $k_{-} = 0$, the integrand of the k_{-} -integral in Eq. (29) or the sum of these two residues times k_{-} is exactly zero. Therefore, we consider only the remaining case $K \geq 0$, where only two poles k_{1-} and k_{2+} have positive imaginary parts. Multiplying Eq. (140) by k_{-} , applying $\lim_{\delta \rightarrow 0}$, and using residues (147) and (148) yields

$$\lim_{\delta \rightarrow 0} k_{-} \int_{-\infty}^{\infty} dk_{+} \tilde{h}_{\pm}(k_{+}) = 2\pi i \frac{h_{\pm}(-2\sqrt{K} + k_{-}) - h_{\pm}(2\sqrt{K} - k_{-})}{\sqrt{K} (2\sqrt{K} - k_{-})}. \quad (150)$$

Inserting this result of the k_{+} -integral in Eq. (29) and carrying the simple integration over k_{-} yields the desired result ($n = n_1 = n_2 \geq n_0$ for $K \geq 0$)

$$\lim_{\rho \rightarrow \infty} J_{\pm}(\rho, t) = \pi \sum_{n \geq n_0}^{\infty} \int_{-\infty}^{\infty} dk_y \int_{-\infty}^{\infty} dk_z \frac{h_{\pm}(2\sqrt{K}) - h_{\pm}(-2\sqrt{K})}{K}, \quad (151)$$

where $K = 2(n - n_0)\omega - k_y^2 - k_z^2 = k_n^2 - k_y^2 - k_z^2$, cf. Eq. (32).

APPENDIX 4

Here, we derive the wavefunction in momentum representation $\tilde{\varphi}_{lm}(\mathbf{v}_{\pm}(t_i))$. Using Fourier transformation (8), wavefunction in coordinate representation $\varphi_{lm}(\mathbf{r})$ (62), spherical harmonics $Y_{lm}(\theta_r, \phi_r)$ (63), and equation for $-i\mathbf{v}_{\pm}(t_i)\mathbf{r}$ (64), we obtain

$$\begin{aligned} \tilde{\varphi}_{lm}(\mathbf{v}_{\pm}(t_i)) &= \frac{C_{\kappa l} \sqrt{\kappa}}{(2\pi)^{3/2}} \sqrt{\frac{2l+1}{4\pi} \frac{(l-m)!}{(l+m)!}} \int_0^{\infty} dr r e^{-\kappa r} \\ &\int_0^{\pi} d\theta_r \sin \theta_r e^{-iv_{\pm}(t_i)r \cos \theta_{v_{\pm}(t_i)} \cos \theta_r} P_l^m(\cos \theta_r) \\ &\int_0^{2\pi} d\phi_r e^{im\phi_r} e^{-iv_{\pm}(t_i)r \sin \theta_{v_{\pm}(t_i)} \sin \theta_r \cos(\phi_{v_{\pm}(t_i)} - \phi_r)}. \end{aligned} \quad (152)$$

Using the substitution $\phi' = \phi_r - \phi_{v_{\pm}(t_i)} - \pi/2$, we get $\cos(\phi_{v_{\pm}(t_i)} - \phi_r) = -\sin \phi'$ and $d\phi_r = d\phi'$. With the help of the Bessel function of the first kind (123), we evaluate the

ϕ' -integral as

$$\begin{aligned} \tilde{\varphi}_{lm}(\mathbf{v}_{\pm}(t_i)) &= C_{\kappa l} \sqrt{\frac{\kappa}{2\pi}} \sqrt{\frac{2l+1}{4\pi} \frac{(l-m)!}{(l+m)!}} e^{im\phi_{v_{\pm}(t_i)}} e^{-im\pi/2} \int_0^{\infty} dr r e^{-\kappa r} \\ &\int_0^{\pi} d\theta_r \sin \theta_r e^{-iv_{\pm}(t_i)r \cos \theta_{v_{\pm}(t_i)} \cos \theta_r} P_l^m(\cos \theta_r) J_m(v_{\pm}(t_i)r \sin \theta_{v_{\pm}(t_i)} \sin \theta_r). \end{aligned} \quad (153)$$

Using Eqs. (19) and (23) of Ref. [29], the θ_r -integral is evaluated as

$$\begin{aligned} &\int_0^{\pi} d\theta_r \sin \theta_r e^{-iv_{\pm}(t_i)r \cos \theta_{v_{\pm}(t_i)} \cos \theta_r} P_l^m(\cos \theta_r) J_m(v_{\pm}(t_i)r \sin \theta_{v_{\pm}(t_i)} \sin \theta_r) \\ &= \sqrt{\frac{2\pi}{v_{\pm}(t_i)r}} e^{-i(l-m)\pi/2} P_l^m(\cos \theta_{v_{\pm}(t_i)}) J_{l+1/2}(v_{\pm}(t_i)r), \end{aligned} \quad (154)$$

hence

$$\tilde{\varphi}_{lm}(\mathbf{v}_{\pm}(t_i)) = C_{\kappa l} \sqrt{\frac{\kappa}{v_{\pm}(t_i)}} Y_{lm}(\theta_{v_{\pm}(t_i)}, \phi_{v_{\pm}(t_i)}) e^{-il\pi/2} \int_0^{\infty} dr \sqrt{r} e^{-\kappa r} J_{l+1/2}(v_{\pm}(t_i)r), \quad (155)$$

cf. Eq. (65). With the Taylor expression of the Bessel function of the first kind

$$J_{\alpha}(x) = \sum_{\beta=0}^{\infty} \frac{(-1)^{\beta}}{\beta! \Gamma(\alpha + \beta + 1)} \left(\frac{x}{2}\right)^{\alpha+2\beta}, \quad (156)$$

we have

$$\begin{aligned} \tilde{\varphi}_{lm}(\mathbf{v}_{\pm}(t_i)) &= C_{\kappa l} \sqrt{\frac{\kappa}{v_{\pm}(t_i)}} Y_{lm}(\theta_{v_{\pm}(t_i)}, \phi_{v_{\pm}(t_i)}) e^{-il\pi/2} \\ &\sum_{\beta=0}^{\infty} \frac{(-1)^{\beta}}{\beta! \Gamma(\beta + l + 3/2)} \left(\frac{v_{\pm}(t_i)}{2}\right)^{2\beta+l+1/2} \int_0^{\infty} dr r^{2\beta+l+1} e^{-\kappa r}. \end{aligned} \quad (157)$$

Using the definition of the Gamma function ($z > 0$)

$$\Gamma(z) = \int_0^{\infty} dx x^{z-1} e^{-x}, \quad (158)$$

the r -integration is easily carried out

$$\int_0^{\infty} dr r^{2\beta+l+1} e^{-\kappa r} = \frac{\Gamma(2\beta + l + 2)}{\kappa^{2\beta+l+2}}, \quad (159)$$

hence

$$\begin{aligned} \tilde{\varphi}_{lm}(\mathbf{v}_{\pm}(t_i)) &= \frac{C_{\kappa l}}{\sqrt{2\kappa^3}} \left(\frac{v_{\pm}(t_i)}{2\kappa} \right)^l Y_{lm}(\theta_{v_{\pm}(t_i)}, \phi_{v_{\pm}(t_i)}) e^{-il\pi/2} \\ &\quad \sum_{\beta=0}^{\infty} \frac{1}{\beta!} \frac{\Gamma(2\beta + l + 2)}{\Gamma(\beta + l + 3/2)} \left(-\frac{v_{\pm}(t_i)^2}{4\kappa^2} \right)^{\beta}. \end{aligned} \quad (160)$$

Using the duplication formula for the Gamma function

$$\Gamma(2z) = \frac{\Gamma(z)\Gamma(z + 1/2)}{2^{1-2z}\sqrt{\pi}} \quad (161)$$

for $z = \beta + l/2 + 1$ yields

$$\begin{aligned} \tilde{\varphi}_{lm}(\mathbf{v}_{\pm}(t_i)) &= C_{\kappa l} \sqrt{\frac{2}{\pi\kappa^3}} \left(\frac{v_{\pm}(t_i)}{\kappa} \right)^l Y_{lm}(\theta_{v_{\pm}(t_i)}, \phi_{v_{\pm}(t_i)}) e^{-il\pi/2} \\ &\quad \sum_{\beta=0}^{\infty} \frac{1}{\beta!} \frac{\Gamma(\beta + l/2 + 1)\Gamma(\beta + l/2 + 3/2)}{\Gamma(\beta + l + 3/2)} \left(-\frac{v_{\pm}(t_i)^2}{\kappa^2} \right)^{\beta}. \end{aligned} \quad (162)$$

Using the Gaussian hypergeometric series

$${}_2F_1(a, b; c; z) = \frac{\Gamma(c)}{\Gamma(a)\Gamma(b)} \sum_{\beta=0}^{\infty} \frac{\Gamma(\beta + a)\Gamma(\beta + b)}{\Gamma(\beta + c)} \frac{z^{\beta}}{\beta!} \quad (163)$$

and Eq. (161) for $z = l/2 + 1$, we obtain

$$\begin{aligned} \tilde{\varphi}_{lm}(\mathbf{v}_{\pm}(t_i)) &= \frac{C_{\kappa l}}{\sqrt{2\kappa^3}} \left(\frac{v_{\pm}(t_i)}{2\kappa} \right)^l Y_{lm}(\theta_{v_{\pm}(t_i)}, \phi_{v_{\pm}(t_i)}) e^{-il\pi/2} \\ &\quad \frac{\Gamma(l + 2)}{\Gamma(l + 3/2)} {}_2F_1\left(\frac{l}{2} + 1, \frac{l}{2} + \frac{3}{2}; l + \frac{3}{2}; -\frac{v_{\pm}(t_i)^2}{\kappa^2}\right), \end{aligned} \quad (164)$$

cf. Eq. (66). Using Euler's hypergeometric transformation

$${}_2F_1(a, b; c; z) = (1 - z)^{c-a-b} {}_2F_1(c - a, c - b; c; z), \quad (165)$$

the wavefunction is then rewritten as

$$\begin{aligned} \tilde{\varphi}_{lm}(\mathbf{v}_{\pm}(t_i)) &= \frac{C_{\kappa l}}{v_{\pm}(t_i)^2 + \kappa^2} \sqrt{\frac{2\kappa}{\pi}} \left(\frac{v_{\pm}(t_i)}{\kappa} \right)^l Y_{lm}(\theta_{v_{\pm}(t_i)}, \phi_{v_{\pm}(t_i)}) e^{-il\pi/2} \\ &\quad \frac{\sqrt{\pi}}{2^{l+1}} \frac{\Gamma(l + 2)}{\Gamma(l + 3/2)} {}_2F_1\left(\frac{l}{2} + \frac{1}{2}, \frac{l}{2}; l + \frac{3}{2}; -\frac{v_{\pm}(t_i)^2}{\kappa^2}\right), \end{aligned} \quad (166)$$

cf. Eq. (67). With the Gaussian theorem for hypergeometric series

$${}_2F_1(a, b; c; 1) = \frac{\Gamma(c)\Gamma(c-a-b)}{\Gamma(c-a)\Gamma(c-b)} \quad (167)$$

and Eq. (161) for $z = l/2 + 1$, the series in Eq. (166) is convergent for $v_{\pm}(t_i)^2 = -\kappa^2$, i.e.

$${}_2F_1\left(\frac{l}{2}, \frac{l}{2} + \frac{1}{2}; l + \frac{3}{2}; 1\right) = \frac{2^{l+1}}{\sqrt{\pi}} \frac{\Gamma(l+3/2)}{\Gamma(l+2)}, \quad (168)$$

cf. Eq. (68), therefore the wavefunction in momentum representation (166) has the pole at $v_{\pm}(t_i)^2 = -\kappa^2$.

APPENDIX 5

Using Eqs. (71), (72), and $v_{\rho\pm}(t_i)^2|_{k=k_n} = -(k_z^2 + 2I_p)$, the factor $|e^{im\phi_{v\pm}(t_i)}|_{k=k_n}^2$ for $m = \pm 1$ is rewritten as

$$|e^{im\phi_{v\pm}(t_i)}|_{k=k_n}^2 = |\cos \phi_{v\pm}(t_i) + i \operatorname{sgn}(m) \sin \phi_{v\pm}(t_i)|_{k=k_n}^2 \quad (169)$$

$$= \frac{|v_{x\pm}(t_i) + i \operatorname{sgn}(m)v_{y\pm}(t_i)|_{k=k_n}^2}{k_z^2 + 2I_p}. \quad (170)$$

With Eqs. (60), (61), $k_{\rho} = \sqrt{k^2 - k_z^2}$, and $|e^{im\theta}|^2 = 1$, it becomes

$$|e^{im\phi_{v\pm}(t_i)}|_{k=k_n}^2 = \frac{\left[A_0\chi_n(k_z) \left(1 \mp \operatorname{sgn}(m)\sqrt{1 - 1/\chi_n(k_z)^2}\right) - \sqrt{k_n^2 - k_z^2}\right]^2}{k_z^2 + 2I_p}. \quad (171)$$

Using Eq. (46), we obtain

$$|e^{im\phi_{v\pm}(t_i)}|_{k=k_n}^2 = \frac{\left[A_0^2\chi_n(k_z)^2 \left(1 \mp \operatorname{sgn}(m)\sqrt{1 - 1/\chi_n(k_z)^2}\right) - n\omega\right]^2}{A_0^2\chi_n(k_z)^2 (k_z^2 + 2I_p)}. \quad (172)$$

Using $\gamma^2 = 2I_p/A_0^2$ and Eq. (31), i.e. $n_0\omega = A_0^2/2 + I_p = I_p/\gamma^2 + I_p = I_p(1 + \gamma^2)/\gamma^2$, we obtain the result for $m = \pm 1$

$$|e^{im\phi_{v\pm}(t_i)}|_{k=k_n}^2 = \frac{I_p \left[2\chi_n(k_z)^2 \left(1 \mp \operatorname{sgn}(m)\sqrt{1 - 1/\chi_n(k_z)^2}\right) - (1 + \gamma^2)n/n_0\right]^2}{2\gamma^2\chi_n(k_z)^2 (k_z^2 + 2I_p)}, \quad (173)$$

cf. Eq. (74).

APPENDIX 6

To obtain the simple analytic solution $\zeta_0(\gamma)$ of Eq. (94)

$$\operatorname{artanh}\sqrt{\frac{\zeta_0^2 + \gamma^2}{1 + \gamma^2}} = \frac{1}{1 - \zeta_0}\sqrt{\frac{\zeta_0^2 + \gamma^2}{1 + \gamma^2}}, \quad (174)$$

in the adiabatic limit $\gamma \ll 1$, we use power series

$$\zeta_0(\gamma) = \sum_{i=0}^{\infty} c_i \gamma^i, \quad (175)$$

yielding

$$\operatorname{artanh}\sqrt{\frac{(\sum_{i=0}^{\infty} c_i \gamma^i)^2 + \gamma^2}{1 + \gamma^2}} - \frac{1}{1 - \sum_{i=0}^{\infty} c_i \gamma^i} \sqrt{\frac{(\sum_{i=0}^{\infty} c_i \gamma^i)^2 + \gamma^2}{1 + \gamma^2}} = 0. \quad (176)$$

In the Taylor series of Eq. (176) at $\gamma = 0$, each coefficient of powers γ^i must be zero. For zeroth order, we get

$$\operatorname{artanh} c_0 - \frac{c_0}{1 - c_0} = 0, \quad (177)$$

with the solution $c_0 = 0$. The coefficient for the first order is then automatically zero. For the second order, we get

$$\frac{c_1(1 + c_1^2)}{\sqrt{1 + c_1^2}} = 0, \quad (178)$$

thus $c_1 = 0$. For other orders, we get

$$\frac{1}{3} - c_2 = 0 \quad (179)$$

$$c_3 = 0 \quad (180)$$

$$\frac{28}{135} + c_4 = 0, \quad (181)$$

thus $c_2 = 1/3$, $c_3 = 0$, and $c_4 = -28/135$. The solution of Eq. (94) is therefore

$$\zeta_0(\gamma) = \frac{\gamma^2}{3} \left(1 - \frac{28}{45} \gamma^2 + \frac{236}{567} \gamma^4 - \frac{5212}{18225} \gamma^6 + \frac{12570692}{63149625} \gamma^8 - \dots \right) \quad (182)$$

and for small $\gamma \ll 1$

$$\zeta_0(\gamma) \approx \frac{\gamma^2}{3}. \quad (183)$$

-
- [1] L. V. Keldysh, Sov. Phys. JETP **20**, 1307 (1965).
- [2] P. Eckle, M. Smolarski, P. Schlup, J. Biegert, A. Staudte, M. Schöffler, H. G. Müller, R. Dörner, and U. Keller, Nature Phys. **4**, 565 (2008).
- [3] P. Eckle, A. N. Pfeiffer, C. Cirelli, A. Staudte, R. Dörner, H. G. Müller, M. Büttiker, and U. Keller, Science **322** 1525, (2008).
- [4] H. Akagi, T. Otobe, A. Staudte, A. Shiner, F. Turner, R. Dörner, D. M. Villeneuve, and P. B. Corkum, Science **325**, 1364 (2009).
- [5] R. Torres, T. Siegel, L. Brugnera, I. Procino, J. G. Underwood, C. Altucci, R. Velotta, E. Springate, C. Froud, I. C. E. Turcu, M. Yu. Ivanov, O. Smirnova, and J. P. Marangos, Opt. Express **18**, 3174 (2010).
- [6] A. P. Pfeiffer, C. Cirelli, M. Smolarski, R. Dörner, and U. Keller, Nature Phys. **7**, 428 (2011).
- [7] A. P. Pfeiffer, C. Cirelli, M. Smolarski, D. Dimitrovski, M. Abu-samha, L. B. Madsen, and U. Keller, Nature Phys. **8**, 76 (2012).
- [8] M. Yu. Ivanov, M. Spanner, and O. Smirnova, J. Mod. Opt. **52**, 165 (2005).
- [9] G. L. Yudin and M. Yu. Ivanov, Phys. Rev. A **64**, 013409 (2001).
- [10] I. Barth and O. Smirnova, Phys. Rev. A **84**, 063415 (2011), Errata: Phys. Rev. A **85**, 029906(E) (2012), Phys. Rev. A **85**, 039903(E) (2012).
- [11] T. Herath, L. Yan, S. K. Lee, and W. Li, Phys. Rev. Lett. **109**, 043004 (2012).
- [12] A. M. Perelomov, V. S. Popov, and M. V. Terent'ev, Sov. Phys. JETP **23**, 924 (1966).
- [13] A. M. Perelomov, V. S. Popov, and M. V. Terent'ev, Sov. Phys. JETP **24**, 207 (1967).
- [14] A. M. Perelomov and V. S. Popov, Sov. Phys. JETP **25**, 336 (1967).
- [15] S. V. Popruzhenko, V. D. Mur, V. S. Popov, and D. Bauer, Phys. Rev. Lett. **101**, 193003 (2008).
- [16] L. Torlina and O. Smirnova, Phys. Rev. A **86**, 043408 (2012).
- [17] J. Kaushal and O. Smirnova, Phys. Rev. A, submitted.
- [18] E. V. Koryukina, J. Phys. B **38**, 3296 (2005).
- [19] M. V. Frolov, N. L. Manakov, E. A. Pronin, and A. F. Starace, Phys. Rev. Lett. **91**, 053003 (2003).
- [20] M. V. Frolov, N. L. Manakov, E. A. Pronin, and A. F. Starace, J. Phys. B **36**, L419 (2003).

- [21] D. Bauer, D. B. Milošević, and W. Becker, *Phys. Rev. A* **72**, 023415 (2005).
- [22] O. Smirnova, M. Spanner, and M. Ivanov, *J. Mod. Opt.* **54**, 1019 (2007).
- [23] J. H. Bauer, *Phys. Rev. A* **83**, 035402 (2011).
- [24] J. H. Bauer, *Phys. Rev. A* **84**, 025403 (2011).
- [25] G. F. Gribakin and M. Y. Kuchiev, *Phys. Rev. A* **55**, 3760 (1997).
- [26] I. Barth and J. Manz, *Phys. Rev. A* **75**, 012510 (2007).
- [27] I. Barth and J. Manz, in *Progress in Ultrafast Intense Laser Science VI*, edited by K. Yamanouchi, A.D. Bandrauk, and G. Gerber, Springer Series in Chemical Physics Vol. 99 (Springer, Berlin, 2010).
- [28] E. Goulielmakis, Z.-H. Loh, A. Wirth, R. Santra, N. Rohringer, V. S. Yakovlev, S. Zherebtsov, T. Pfeifer, A. M. Azzeer, M. F. Kling, S. R. Leone, and F. Krausz, *Nature* **466**, 739 (2010).
- [29] A. A. R. Neves, L. A. Padilha, A. Fontes, E. Rodriguez, C. H. B. Cruz, L. C. Barbosa, and C. L. Cesar, *J. Phys. A* **39**, L293 (2006).
- [30] I. Barth and O. Smirnova, in preparation.
- [31] V. M. Rylyuk and J. Ortner, *Phys. Rev. A* **67**, 013414 (2003).
- [32] V. M. Rylyuk, *Phys. Rev. A* **86**, 013402 (2012).

FIGURE CAPTIONS

FIG. 1: Time-averaged ionization rates $w_+(\mathcal{E}, \omega)$ for s (orange), p_0 (green), p_+ (blue), p_- (red) orbitals and right circular polarization versus laser frequency ω for $I_p = 0.5$ a.u. and laser amplitude $\mathcal{E} = 0.06$ a.u. The solid, dashed, and dotted curves correspond to the accurate (Eqs. (76)–(78)), approximate (Eqs. (88)–(90)), and simple (Eqs. (100)–(102)) results, respectively. Note that $|C_{\kappa l}|^2 = 1$ are used.

FIG. 2: Time-averaged ionization rates $w_+(\mathcal{E}, \omega)$ for s (orange), p_0 (green), p_+ (blue), p_- (red) orbitals and right circular polarization versus laser intensity $I = c^2 \epsilon_0^2 \mathcal{E}^2$ for $I_p = 0.5$ a.u. and laser frequency $\omega = 0.057$ a.u. (800 nm) in logarithmic scale. The solid curves corresponds to the accurate results (Eqs. (76)–(78)). Because of the logarithmic scale, the accurate (Eqs. (76)–(78)), approximate (Eqs. (88)–(90)), and simple (Eqs. (100)–(102)) results coincide within graphical resolution. Note that $|C_{\kappa l}|^2 = 1$ are used.

FIG. 3: Time-averaged n -photon ionization rates $w_{n+}(\mathcal{E}, \omega)$ (Eq. (36)) or equivalently photoelectron energy distribution at the detector for s (orange), p_0 (green), p_+ (blue), p_- (red), and total p (brown) orbitals and right circular polarization versus final electronic kinetic energy $k_n^2/2$ (Eq. (37)) for $I_p = 0.5$ a.u., laser amplitude $\mathcal{E} = 0.06$ a.u., and laser frequency $\omega = 0.057$ a.u. (800 nm). The solid and dashed curves correspond to the accurate (Eqs. (76)–(78)) and approximate (Eqs. (88)–(90)) results, respectively. The spectra for total p orbitals are calculated according to $w_{n+}^p(\mathcal{E}, \omega) = w_{n+}^{p_0}(\mathcal{E}, \omega) + w_{n+}^{p_+}(\mathcal{E}, \omega) + w_{n+}^{p_-}(\mathcal{E}, \omega)$. Note that $|C_{\kappa l}|^2 = 1$ are used. The approximate results of the ionization rates for p_+ and p_- orbitals are equal at the final kinetic energy $2U_p + I_p \approx 1.05$ a.u, see text for discussion. In the adiabatic limit $\gamma \ll 1$, all photoelectron distributions are peaked at $2U_p \approx 0.55$ a.u. and are the same for p_+ and p_- orbitals.

FIGURES

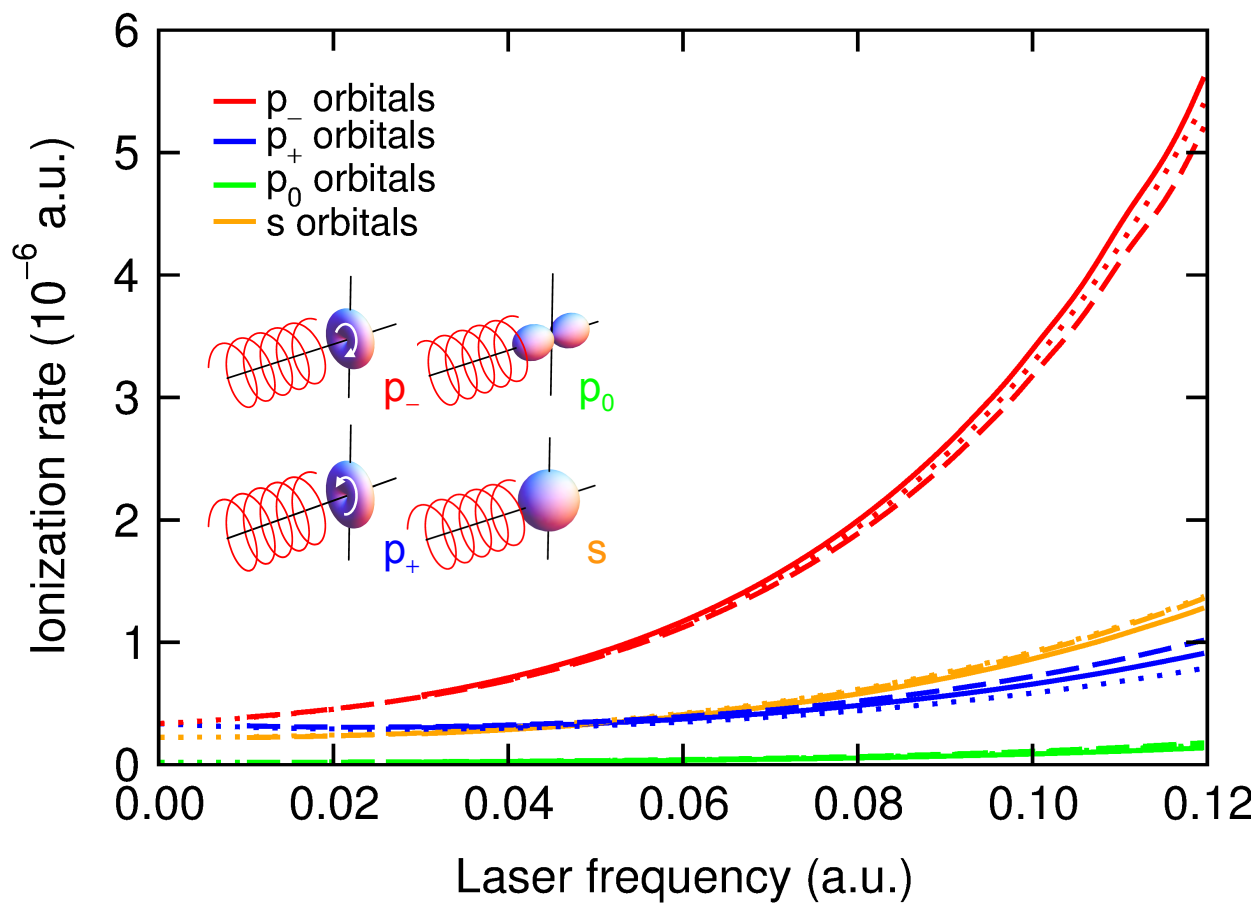


FIG. 1.

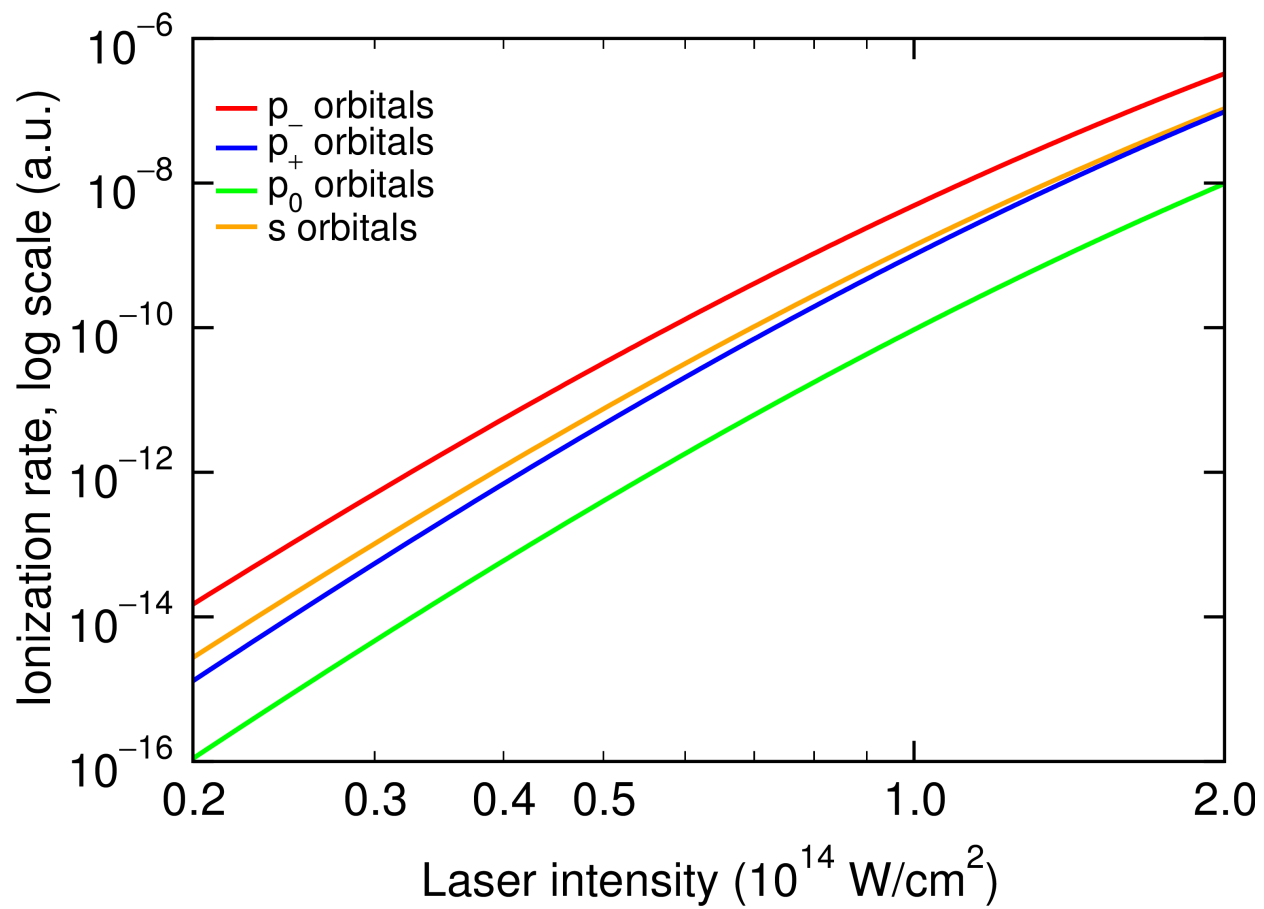


FIG. 2.

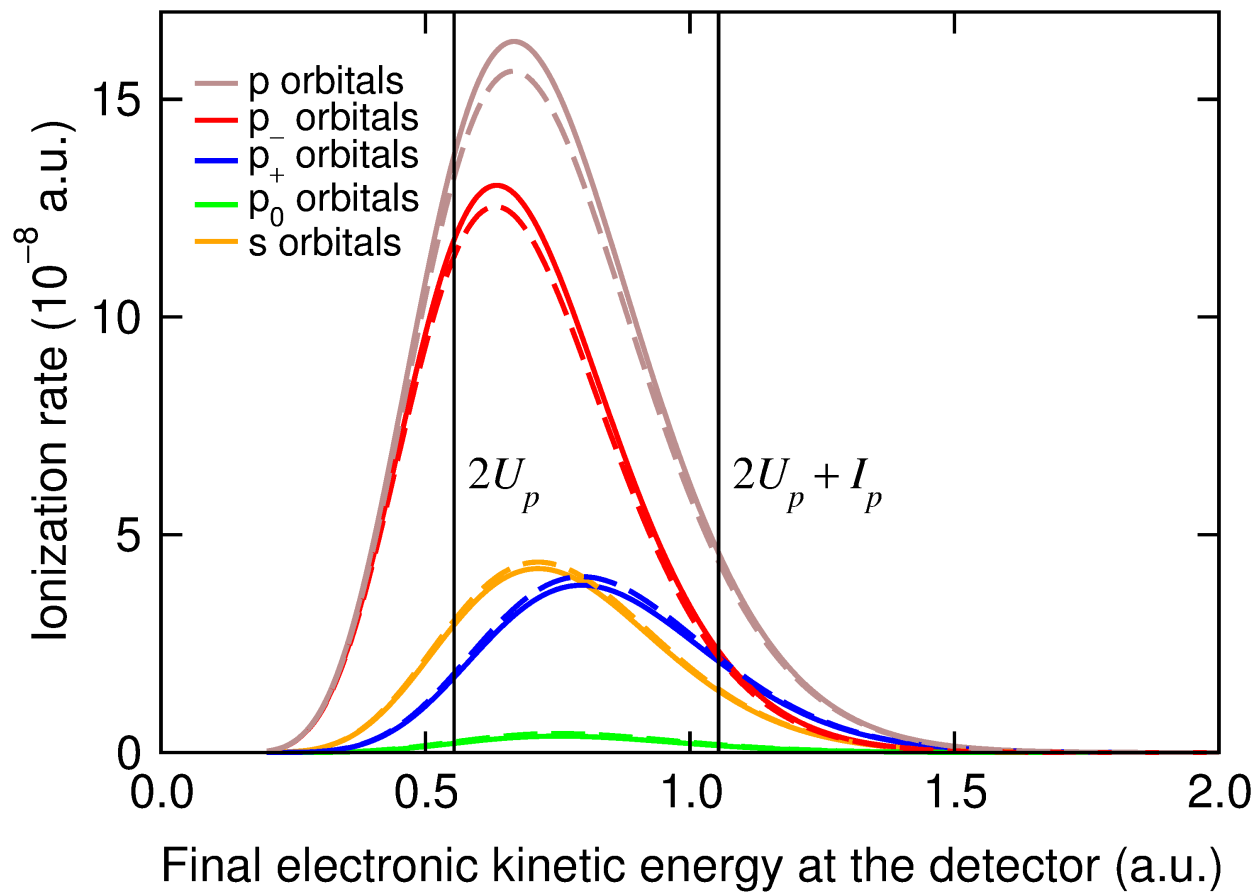


FIG. 3.